

THESIS FOR THE DEGREE OF LICENTIATE OF ENGINEERING

# Lean NO<sub>x</sub> reduction over Ag/Al<sub>2</sub>O<sub>3</sub> catalysts using future fuels

Effects of ageing and catalyst composition

FREDRIK K. GUNNARSSON

Department of Chemical and Biological Engineering

CHALMERS UNIVERSITY OF TECHNOLOGY

Gothenburg, Sweden 2013



**CHALMERS**



# CHALMERS

Lean NO<sub>x</sub> reduction over Ag/Al<sub>2</sub>O<sub>3</sub> catalysts using future fuels  
Effects of ageing and catalyst composition  
FREDRIK K. GUNNARSSON

© FREDRIK K. GUNNARSSON, 2013.

Licentiatuppsats vid Institutionen för kemi- och bioteknik  
Chalmers tekniska högskola  
Serie nr. 2013:7  
ISSN 1652:943X

Department of Chemical and Biological Engineering  
Chalmers University of Technology  
SE-412 96 Gothenburg  
Sweden  
Telephone + 46 (0)31-772 1000

Chalmers Reproservice  
Gothenburg, Sweden 2013

# **Lean NO<sub>x</sub> reduction over Ag/Al<sub>2</sub>O<sub>3</sub> catalysts using future fuels**

## **Effects of ageing and catalyst composition**

FREDRIK GUNNARSSON

Department of Chemical and Biological Engineering

Chalmers University of Technology, Göteborg 2013.

### **Abstract**

The focus of this work is to increase the understanding of the lean NO<sub>x</sub> reduction over silver-alumina catalysts using hydrocarbons as the reductant (HC-SCR). In particular, the effect of silver loading, the role of platinum doping, the effect of the reducing agent as well as the effects of aging and hydrothermal treatment on the catalytic activity, in particular at low temperatures, and selectivity, were investigated. Silver-alumina samples were prepared using a sol-gel method, including freeze-drying, and evaluated for HC-SCR. The samples were synthesized with varying silver loading, with and without addition of trace amounts of platinum. Activity studies, hydrothermal treatment and oxidation experiments were performed in a synthetic gas-bench reactor using model hydrocarbons (n-octane, ethane, ethane, ethyne) and a commercial bio-diesel (NExBTL) as the reducing agent. The samples were characterized with respect to surface area (BET) and nature and relative amount of surface silver species (UV-vis, XPS).

The results show that silver-alumina catalysts, prepared via sol-gel synthesis, display a high consistency regarding surface area and the relative amount of different silver species, as the silver loading is varied. It can be seen that activation for oxidation generally proceeds more easily with increasing bond order of the hydrocarbon. Furthermore, the use of hydrocarbons with high bond order, that is ethyne, as reductant for NO<sub>x</sub> results not only in the highest peak activity for lean NO<sub>x</sub> reduction but also in considerable high activity in a wide temperature range mainly thanks to high activity at low temperatures. With increasing silver loading, the oxidation reactions are favored such that both the hydrocarbon and the NO activation occur at lower temperatures. As the hydrocarbon chain-length is increased, the NO<sub>x</sub> reduction decreases, however, high activity can be seen even when using the commercial bio-diesel. For the pure silver-alumina samples tested with NExBTL, the 6 wt% Ag sample displays the highest activity reaching 60% at 350°C.

Furthermore, it is concluded that as the samples are doped with trace-amounts of platinum, the activity for lean NO<sub>x</sub> reduction at low temperatures is enhanced. The catalyst composition showing the highest activity for NO<sub>x</sub> reduction, using n-octane as reducing agent, is found to be a 2 wt% loaded Ag/Al<sub>2</sub>O<sub>3</sub> sample doped with 500 ppm platinum. This catalyst also displays the highest low-temperature activity (51% NO<sub>x</sub> reduction at 300°C), most likely owing to an increased ability to partially oxidize the hydrocarbon reductant as well as higher adsorption of the hydrocarbon on the surface, attributed to the Pt doping.

**Keywords:** HC-SCR, Ag/Al<sub>2</sub>O<sub>3</sub>, bio-fuels, Pt-doping, catalyst ageing

## List of Publications

This thesis is based on the following publications, I-III:

### **I. Influence of ageing, silver loading and type of reducing agent on the lean NO<sub>x</sub> reduction over Ag-Al<sub>2</sub>O<sub>3</sub> catalysts**

Fredrik Gunnarsson, Jenny-Yue Zheng, Hannes Kannisto, Clément Cid, Anna Lindholm, Mirosława Milh, Magnus Skoglundh and Hanna Härelind

Accepted for publication in *Topics in Catalysis* (2012)

### **II. Improved low temperature activity of Ag-alumina for lean NO<sub>x</sub> reduction – effects of Ag loading and low level Pt doping.**

Fredrik Gunnarsson, Hannes Kannisto, Magnus Skoglundh and Hanna Härelind

Submitted for publication to *Applied Catalysis B: Environmental* (2013)

### **III. Influence of the Carbon–Carbon Bond Order and Silver Loading on the Formation of Surface Species and Gas Phase Oxidation Products in Absence and Presence of NO<sub>x</sub> over Silver-Alumina Catalysts**

Hanna Härelind, Fredrik Gunnarsson, Seyyed Majid Sharif Vaghefi, Magnus Skoglundh, and Per-Anders Carlsson.

*ACS Catalysis*, 2 (2012) 1615

## Contribution report

- I. Responsible for the experimental work and analysis regarding the reducing agent and hydrothermal treatment study as well as writing of the manuscript.
- II. Responsible for all experimental and analytic work as well as writing of the manuscript.
- III. Responsible for flow-reactor experiments and catalyst synthesis.

## Table of Contents

1. Introduction.....	7
1.1. Selective Catalytic Reduction.....	7
1.2. The silver alumina system .....	8
1.3. Deactivation.....	9
1.4. Objectives.....	10
2. Experimental methods .....	11
2.1. Catalyst preparation .....	11
2.1.1. Sol-gel.....	11
2.1.2. Freeze-drying.....	11
2.1.3. Calcination .....	11
2.1.4. Monolith coating.....	11
2.2. Catalyst characterization.....	12
2.2.1. Surface area measurements .....	12
2.2.2. X-ray photoelectron spectroscopy .....	12
2.2.3. UV-vis spectroscopy .....	12
2.3. Catalyst performance.....	13
2.3.1. Synthetic gas flow reactor .....	13
3. Results and discussion .....	17
3.1. Active phase characterization.....	17
3.2. Hydrocarbon oxidation .....	19
3.3. NO <sub>x</sub> reduction activity .....	24
4. Conclusions.....	29
5. Outlook .....	31
6. Acknowledgements.....	33
7. List of abbreviations .....	35
8. References .....	37



## 1. Introduction

As the market becomes increasingly globalized, the need for transport has increased steadily over the last century. In 1990 the number of cars, motorcycles, busses and trucks in the world was estimated to 650 million [1]. Although extensive research is performed on alternative propulsion systems, the combustion engine will probably be the most dominant system for automotive propulsion for the coming decennia. The combustion engine has already had major impact on the environment, resulting in ever more stringent emission legislation regarding both the emissions of CO and CO<sub>2</sub> as well as the emissions of more directly harmful gases, *i.e.* nitrogen oxides (NO<sub>x</sub>), particulate matter and unburned fuel [2, 3]. These emission legislations and limited resources of fossil fuels are strong drivers for energy-efficient engine concepts, such as diesel and lean-burn engines [4], which reduce the fuel consumption and thereby also the emissions of CO<sub>2</sub> as compared to stoichiometric gasoline engines. Emissions of NO<sub>x</sub> are hazardous to the environment, acting as a source to ground level ozone, acid rain and eutrophication, as well as being directly harmful to humans. The legislated emission levels of NO<sub>x</sub> for heavy-duty vehicles have decreased from 8.0 g/kWh in 1992 (Euro I), to 0.4 g/kWh in the coming Euro VI levels, which are to be implemented in 2013 [4]. Solving the problem of NO<sub>x</sub> emission abatement is therefore of crucial importance. The conventional way of reducing NO<sub>x</sub> emissions has been by the use of a three-way-catalyst (TWC). The catalyst consists of noble metals (platinum, palladium and rhodium) supported on alumina ( $\gamma$ -Al<sub>2</sub>O<sub>3</sub>) and has the ability to simultaneously oxidize CO and unburned hydrocarbons while also reducing the NO<sub>x</sub>. However, the lean environment in the exhaust gas from new engine systems, with high air-to-fuel ratios, obstructs the NO<sub>x</sub> reduction in the TWC, which needs to operate closer to stoichiometric ( $A/F= 14.7$ ) air-to-fuel ratio [5]. In addition to increasing the air-to-fuel ratio, the new engine systems also operate at much lower temperatures, resulting in exhaust temperatures as low as 150°C, which is a true challenge when designing alternative catalyst techniques.

A number of new technics have been developed in order to decrease the emission of NO<sub>x</sub>. One example is exhaust gas recirculation (EGR) where the inlet air to the combustion chamber is mixed with exhaust gases, lowering the oxygen concentration in the combustion chamber and thereby lowering the amount of formed NO<sub>x</sub> [6]. Other techniques are NO<sub>x</sub> storage catalysts where the engine is run at alternating lean and rich phases, storing NO<sub>x</sub> during the lean phase and then reducing the stored NO<sub>x</sub> during the shorter rich phase [5, 7-9] and selective catalytic reduction (SCR), using either hydrocarbons or ammonia from urea as reducing agent. The focus of the present work is selective catalytic reduction of NO<sub>x</sub> over silver alumina catalysts using hydrocarbons, *i.e.* fuel, (HC-SCR), as the reducing agent.

### 1.1. Selective Catalytic Reduction

Selective catalytic reduction of NO<sub>x</sub> is a promising technique which circumvents the TWC-problem. The urea-SCR technique is already implemented in large parts of the industrialized world, both in the automotive industry and in stationary applications. However, although urea solutions for the automotive industry, *e.g.* AdBlue and DEF, are readily available in many countries, *e.g.* USA and large parts of Europe, access to urea is still very limited in the larger part of the world [10]. An advantage with the HC-SCR system is that as the fuel is used as

reducing agent, no additional component is needed and the system can be utilized for all automotives world-wide. The concept of selectively reducing NO<sub>x</sub> using hydrocarbon as the reducing agent was first introduced in 1990 by Iwamoto *et al.* [11] and Held *et al.* [12], both showing independently that the presence of hydrocarbons enhanced the lean NO<sub>x</sub> reduction over Cu-ZSM5 catalysts. These catalysts were however found to be sensitive to water. Subsequently, catalysts with higher tolerance to hydrothermal conditions were investigated, discussed in detail by Burch [13]. In 1993, Miyadere showed very high activity for NO<sub>x</sub> reduction, as compared to previous studies, over silver supported on alumina in the presence of water [14]. The Ag-alumina system is described in section 1.2.

The main reactions in HC-SCR are the NO<sub>x</sub> reduction, facilitated by the hydrocarbon reductant, and the competing combustion reaction, where the hydrocarbon is oxidized by the oxygen. The NO<sub>x</sub> reduction reaction is divided into three main reactions: I) the oxidation of NO to NO<sub>2</sub> and the formation of surface nitrates and nitrites, II) the adsorption of hydrocarbons onto the surface and the partial oxidation of the hydrocarbons forming various oxygenated carbon surface species and III) the reaction between the partially oxidized hydrocarbons and the surface nitrogen containing species, forming N<sub>2</sub>, CO<sub>2</sub> and water [13].

One of the main steps thought to be crucial for achieving high performance at low temperature is the activation of the hydrocarbon, *i.e.* the partial oxidation, before it reacts with the NO<sub>x</sub> to form N<sub>2</sub> [15, 16]. Burch *et al.* [17] and Arve *et al.* [18] have proposed that the initial step in hydrocarbon activation is the dissociation of the first hydrogen from the hydrocarbon reductant. The dissociation is related to the sticking probability which is proportionally dependent on the sticking coefficient and exponentially dependent on the dissociative chemisorption energy of the molecule on the surface [1]. The oxidation properties of the active phase and the dissociative chemisorption energy for the hydrocarbon on the surface are therefore of crucial importance and need to be tuned so that it only partially oxidizes the hydrocarbon without combusting it.

## 1.2. The silver alumina system

Silver-alumina (Ag/Al<sub>2</sub>O<sub>3</sub>) has been pointed out as a potential catalyst for lean NO<sub>x</sub> reduction, displaying promising results for a variety of hydrocarbons, including fossil fuels and bio-fuels [19-24]. One drawback with the Ag/Al<sub>2</sub>O<sub>3</sub> system has been that the system requires relatively high temperatures to achieve high activity, while as the energy efficiency in engines increases, the exhaust gas temperature decreases. Many new engine designs also include heat recovery systems which decrease the exhaust temperature in the catalyst even further. Nevertheless, the active temperature window for HC-SCR over Ag/Al<sub>2</sub>O<sub>3</sub> may be shifted towards lower temperatures, provided a small amount of hydrogen is introduced to the exhaust feed [25-28]. The addition of hydrogen further results in an over-all increase in the NO<sub>x</sub> reduction. The 2 wt% Ag/Al<sub>2</sub>O<sub>3</sub> system has shown high NO<sub>x</sub> reduction activity in the presence of hydrogen [23, 28-30]. The added hydrogen does however increase the fuel-penalty, as it is produced from on-board fuel-reforming. Recently Kannisto *et al.* have showed that hydrogen levels as low as 1000 ppm result in a fuel penalty of about 2% [31], cf. 0.5% for urea-SCR.

As mentioned previously, the main reactions in HC-SCR are the NO<sub>x</sub> reduction, by the hydrocarbon, and the competing reaction where the hydrocarbon is oxidized by the oxygen, *i.e.* combusted. To favor the desired reduction reaction and to reach a good low-temperature performance, the hydrocarbon needs to be activated, *i.e.* partially oxidized, before reacting

with the  $\text{NO}_x$  [15-19]. This can be achieved by various routes, likely including several active sites. Although the complete reaction mechanism over  $\text{Ag}/\text{Al}_2\text{O}_3$  is still under debate, several active sites are likely involved *e.g.* silver ions, small silver clusters and larger metallic silver particles [32-34]. It has for instance been suggested that  $\text{Ag}_n^{\delta+}$  clusters are highly active for the HC-SCR process [35], particularly for the activation of the reducing agent by partial oxidation. It has been shown that very small silver clusters ( $\text{Ag}_n < 8$ ) to a greater extent provide active sites for lean  $\text{NO}_x$  reduction with hydrocarbons as compared to larger silver crystallites [36]. Despite the numerous studies, the structure and chemical state of silver in such clusters remain elusive. For example metallic silver, silver oxides and silver aluminate have all been suggested as the main active phase [13, 36]. It has been shown, however, that different forms of oxidized silver species, like  $\text{Ag}^+$ ,  $\text{Ag}_2\text{O}$ , or silver aluminate, favor the reduction of  $\text{NO}$  to  $\text{N}_2$  [37, 38] whereas metallic silver particles are more active for oxidation reactions [39-41]. These findings indicate that catalysts, that are active for  $\text{NO}_x$  reduction by hydrocarbons most likely contain highly dispersed ionic, oxidized and/or  $\text{Ag}_n^{\delta+}$  silver species. To prevent the competing combustion reaction of hydrocarbon to  $\text{CO}_2$  and  $\text{H}_2\text{O}$ , the oxidation strength of the oxidation sites is of crucial importance, ensuring that the hydrocarbon is only partially oxidized to active surface species. It has also been found that addition of trace amounts of platinum group metals (PGM) to the  $\text{Ag}/\text{Al}_2\text{O}_3$  catalyst may have a beneficial effect on the  $\text{NO}_x$  reduction [31]. The study suggests that platinum acts as an oxidizer, facilitating partial oxidation of the hydrocarbon and making it more readily available for the  $\text{NO}_x$  reduction reaction. The authors do however stress that, as platinum is such a strong oxidizer, it is important to keep a low platinum level to reduce the risk of combusting the reducing agent. Ways to facilitate the partial oxidation of the hydrocarbon may be to incorporate additional oxidation sites in the Ag-alumina catalyst or by altering the oxidizing potential of the existing oxidation sites. Previous studies [31] indicate that trace-amounts of platinum incorporated in the silver-alumina catalyst, increase the maximum  $\text{NO}_x$  reduction and at the same time decrease the onset temperature of the HC-SCR reaction. It has also been proposed that the addition of platinum chloride increases the adsorption of hydrocarbons, which could facilitate a higher  $\text{NO}_x$  reduction activity at low temperature since more hydrocarbons would be available on the surface [42]. The authors ascribe the increase in HC-adsorption to a change in the acidity of the surface due to chlorine residue from the synthesis.

### 1.3. Deactivation

As catalysts does not participate in the reaction as a reactant they should in theory last forever, however many factors contribute to the degradation of a catalyst. These are divided into three major mechanisms: poisoning, fouling and thermal degradation [43]. Poisoning occurs when a material binds strongly to the active sites of a catalyst, preventing the reactants to reach them and thereby inhibiting the catalytic process. Although the poison can be removed in some cases, poisoning is manly an irreversible process. Fouling is similar to poisoning, however fouling is usually reversible. Instead of chemically binding to the active site, a fouling agent physically blocks the surface and the pores, covering the active sites and the active surface area. Thermal degradation can either be derived from alternating heating and cooling the material, resulting in the formation of cracks in the support material and thereby loss of surface area and active material. High temperatures can also result in sintering of small active particles, which then agglomerate, decreasing the active surface area and

thereby the activity of the catalyst. The tolerance towards deactivation in high temperature environment is therefore of great importance.

#### **1.4. Objectives**

The project was performed as a part of the second phase of the Mistra project E4, Energy Efficient Reduction of Exhaust Emissions from Vehicles. The overall goal of the second phase of the MISTRA E4 project is to further improve the applied technologies, secure the functionality and stability of the integrated system, and utilize suitable renewable fuels as alternatives to fossil fuel to decrease the emission of fossil CO<sub>2</sub>.

The objective of this thesis is to increase the understanding of the catalytic process concerning the lean NO<sub>x</sub> reduction over silver-alumina catalysts. In particular, the effect of silver loading, the role of platinum-doping, the effect of the reducing agent as well as the effects of aging and hydrothermal treatment on the catalytic activity, selectivity and low-temperature performance are in focus.

## 2. Experimental methods

### 2.1. Catalyst preparation

#### 2.1.1. Sol-gel

A sol is defined as a solid suspension where the size of the dispersed solid is so small that the particles are kept from sedimenting by Brownian motion.

The Ag/Al<sub>2</sub>O<sub>3</sub> samples were prepared by a sol-gel method including freeze drying [32], with a nominal silver loading of 2, 4 and 6 wt%, respectively (Paper I-III). In addition to the pure Ag-alumina, the corresponding samples were prepared with addition of 100 and 500 ppm platinum. The catalysts are denoted as: Ag(silver loading in %)Pt(platinum doping in ppm) (Paper II). The alumina precursor (aluminum isopropoxide, >98%, Aldrich) was added to milli-Q water and heated to 82°C during vigorous stirring. Subsequently, the silver precursor (AgNO<sub>3</sub>, >99%, Sigma), and for the doped samples a platinum precursor (Pt(NO<sub>3</sub>)<sub>2</sub>, solution type K, Heraeus), was added. The pH was adjusted to 4.5 by addition of HNO<sub>3</sub> (10%, Fluka), resulting in the formation of a sol. The sol was stirred for 12 h, after which a major part of the solvent was removed using a heated vacuum system.

#### 2.1.2. Freeze-drying

When micro-porous materials are thermally dried, localized boiling may occur which can lead to a considerable pressure drop in the micro-porous channels. This can lead to pore collapse which will reduce the surface area of the material. In addition, finely dispersed atoms/clusters may, due to the high temperature, migrate and agglomerate to larger particles. In order to preserve the micro-porous structure of the  $\gamma$ -alumina, the gel can instead be dried using a freeze-drying method, where the solvent is removed via sublimation. This prevents both pore collapse and cluster migration.

The samples were initially frozen using liquid nitrogen. The frozen samples were then subjected to pressures below 5 hPa and -110°C in a Freeze dryer (SCANVAC, CoolSafe 110-4 Pro) resulting in an aerogel.

#### 2.1.3. Calcination

The freeze-dried gel, *i.e.* aero-gel, consisting of aluminumoxyhydroxide, is subsequently heated to 600°C in air where it phase transforms to  $\gamma$ -alumina. The sample is placed in an oven and the temperature is raised at 2°C/min from RT to 600°C. In addition to the solid state reaction, the sample is also purged from undesired compounds such as remaining nitrates and carbon containing species.

#### 2.1.4. Monolith coating

A wash-coat slurry with 20 wt% dry content was prepared, where the dry part consisted of 20 wt% AlOOH-binder (Disperal P2, Condea) and 80 wt% catalyst powder and the solvent consisted of 50% Milli-Q and 50% EtOH. The monolith was submerged in the slurry, dried at

90°C for 15 min and then subjected to a fast calcination at 600°C for 2 minutes. The procedure was repeated until the desired amount of wash-coat was acquired (20% of total weight), where after the monoliths were calcined in air (600°C, 3h).

## **2.2. Catalyst characterization**

### **2.2.1. Surface area measurements**

The total surface area can be determined according to the BET-theory [44], which is based on physical adsorption of gas molecules on a solid surface. The theory assumes that gases adsorb on a solid surface in infinite mono-layers and that there is no interaction between these adsorption layers. The Langmuir isotherm, which relates the coverage of the adsorbate on a solid surface to gas pressure or concentration of a medium above the solid surface at a fixed temperature, is applied and extended to function for several layers.

In practice, physisorption of nitrogen at the condensation temperature of N<sub>2</sub>, i.e. 77 K, is used and by performing measurements at different equilibrium pressures, a linear plot can be derived (adsorbed amount vs. pressure). From the slope and the intercept of this plot, using the known projected area of the nitrogen molecule, calculations using the ideal gas law and Avogadro's constant results in the specific surface area of the investigated material [45].

The measurements were performed using a Micrometrics Tristar 3000 instrument with nitrogen sorption at 77 K (Paper I-III). The samples were dried in vacuum at 225°C for 2 hours before the measurements.

### **2.2.2. X-ray photoelectron spectroscopy**

X-ray photoelectron spectroscopy (XPS) utilizes a highly monochromatic x-ray beam which irradiates the sample and uses the photoelectric effect [1, 46]. The x-rays are absorbed and photoelectrons are emitted. The kinetic energy of the emitted electron is equal to the difference between the energy of the x-rays and the binding energy of the emitted electrons [46]. The intensity of the emitted photoelectrons is measured as a function of the kinetic energy [1] and by varying the energy of the monochromatic incoming x-rays, a spectra of the binding energies is derived. The sample is initially studied with a fast sweep, locating the existing peaks, where after the peaks are studied with eight sweeps in high resolution. As the sample is radiated some charging of the sample may arise. To compensate for this potential charging, all spectra are calibrated with respect to the carbon C 1s peak at 284.5 eV [47]. The experiments in this work (Paper II) were performed using a Perkin-Elmer PHI 5000 C instrument, with a monochromatic Al K<sub>α</sub> source.

### **2.2.3. UV-vis spectroscopy**

The UV-vis spectroscopy gives information about the electronic structure from the absorption bands between ultraviolet and visible light [48]. The information relates to the electronic levels in the atoms, ions, complexes or molecules. When studying solid catalysts, as is the case in the work, the diffuse reflectance from the powder sample is analyzed. This radiation derives from the incoming radiation which is absorbed and then reflected after multiple

scattering. The frequency of the reflected beam relates to the transition energy between different orbitals in the atom.

The fresh and aged 2 and 6 wt% Ag-alumina samples (Paper I) as well as 2 and 6 wt% Ag-alumina samples, pure or doped with 500 ppm (Paper II) were studied using a Varian Cary 5000 UV-vis-NIR spectrophotometer, with Labsphere Spectralon reference.

## 2.3. Catalyst performance

### 2.3.1. Synthetic gas flow reactor

The catalytic performance for lean NO<sub>x</sub> reduction was evaluated at steady-state conditions in a continuous gas flow reactor, Figure 1. The reactor chamber consisted of a horizontally mounted quartz tube (L=80 cm, ID=22 mm), which was heated by a metal coil (PID regulated, Eurotherm) and insulated with quartz-wool. The monolith sample was placed close to the outlet, maximizing the gas heating, with uncoated monoliths before and after to minimize heat-losses from radiation, as described by Kannisto *et al.* [32]. The inlet gas composition, 200 ppm NO, 1000 ppm H<sub>2</sub>, 10 % O<sub>2</sub> and Ar<sub>bal</sub> for Paper I-II and 600 ppm C<sub>2</sub>H<sub>x</sub> (x=2,4 or 6), 200 ppm NO, 10 % O<sub>2</sub> and Ar<sub>bal</sub> for Paper III, was controlled by separate mass flow controllers (Bronkhorst Hi-tech) and the outlet gas composition was analyzed using a FTIR gas-analyzer (MKS 2030 HS). Water (corresponding to 5%) and liquid hydrocarbon (n-octane or NExBTL), used in Paper I and Paper II, were introduced separately to the reactor chamber via controlled evaporator mixer systems (CEM, Bronkhorst Hi-Tech). The total gas flow was 3500 mL/min, resulting in GHSV = 33 200 h<sup>-1</sup>.

In Paper I and II, the catalyst samples were initially conditioned in 10% oxygen and argon at 550°C, after which they were investigated at steady-state conditions for 30 minutes between 400 and 225°C in 25°C steps, using n-octane or a commercial bio-diesel (NExBTL) as reducing agent. The C/N molar ratio was kept constant at 6 during all experiments, corresponding to a C<sub>1</sub>-concentration of 1200 ppm. The Ag<sub>2</sub> and Ag<sub>6</sub> samples in Paper II were also subjected to hydrothermal treatment at 500°C in 10% O<sub>2</sub> and 10% H<sub>2</sub>O, with argon balance, for 12 hours. In Paper III, the catalysts were evaluated using transient (cooling) temperature experiments, with a C/N ratio of 6. Formation of nitrogen containing species, other than NO and NO<sub>2</sub>, *i.e.* NH<sub>3</sub>, HNCO, N<sub>2</sub>O and cyanide species, were monitored and the concentrations were determined to be negligible (well below 5 ppm). Hence these species were excluded from the NO<sub>x</sub> reduction calculations, which were derived in accordance with Eq. 1 and 2.

$$NO_x = NO + NO_2 \quad (1)$$

$$NO_x \text{ reduction } (\%) = 100 * (NO_{x,in} - NO_{x,out}) / NO_{x,in} \quad (2)$$

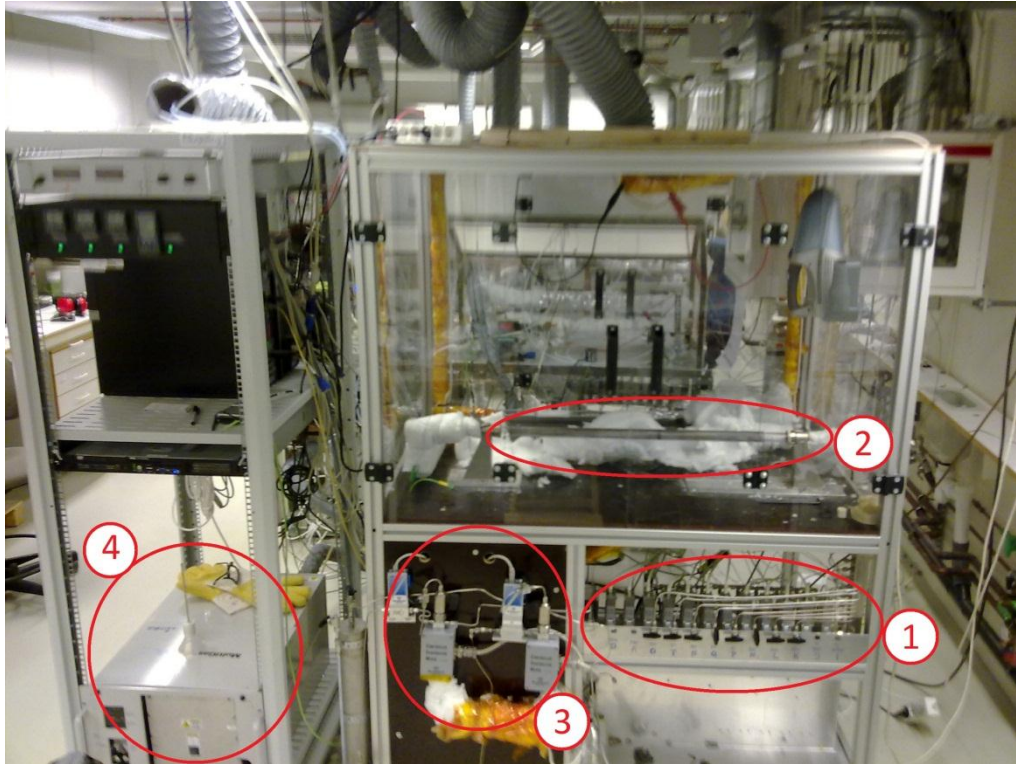


Figure 1: A synthetic gas bench reactor showing 1) MFC-system, 2) reactor chamber, 3) CEM-system and 4) FTIR gas analyser.

The hydrocarbon conversion was determined according to Eq. 3 and 4.

$$C_{1,out} = CO_{out} + CO_{2,out} \quad (3)$$

$$HC \text{ conversion } (\%) = 100 * (C_{1,out} / C_{1,in}) \quad (4)$$

### **Hydrocarbon addition**

The liquid hydrocarbon, in Paper I-II, was introduced via a controlled evaporation mixing (CEM, Brokhors Hi-tech). The system is composed of a liquid mass flow controller and a gas mass flow controller for carrier gas, connected to a small furnace where the HC was vaporized and subsequently feed to the reactor via heated tubes. The reductants used was n-octane, as model hydrocarbon, and commercial bio-diesel, NExBTL, consisting of n- (<10%) and iso- (>90%) paraffins according to the producer. The use of the latter, a biomass-to-liquid product from vegetable oils and animal fats, has been shown to result in reduced engine-out emissions of NO<sub>x</sub>, HC and CO at heavy-duty conditions, when blended with other diesel fuels *e.g.* EN590 and EC1 [49].

## **FTIR**

The outlet concentrations (Paper I-III) were measured using a FTIR gas analyzer (MKS instruments, MultiGas 2030 HS). Fourier transformed infrared spectroscopy is a vibrational spectroscopy which utilizes the infrared region of the electromagnetic spectra [48]. As a sample is subjected to infrared radiation it induces vibrations in the molecular bonds, provided the dipole moment of the molecule changes during the radiation. The vibrations are caused by an overlap between the IR- frequency and the frequency of the molecular bond, especially in the middle region ( $4000\text{-}200\text{ cm}^{-1}$ ) which corresponds to the energy of vibration and translation [48]. A molecule does not have to be a permanent dipole to be IR-active, if a dipole can be induced by the radiation, however symmetrical molecules such as  $\text{O}_2$  and  $\text{N}_2$ , cannot be detected with FTIR [50]. The vibrations correspond to absorption peaks with specific frequencies. A specific molecule bond will have an absorption peak within a certain frequency range depending on its close surrounding. The quantitative concentration of the bond can be determined by measuring the area of the absorption peak [48]. The absorption spectrum is unique for a specific compound, hence qualitative analysis of a compound is possible, however many species have partially overlapping spectra. This may result in difficulties when distinguishing between different compounds hence it is beneficial to have some knowledge about the samples in advance.

The advantage of using FTIR, as compared to conventional infrared spectroscopy, is that FTIR has an interferometer, making it possible to measure all the frequencies in the infrared region simultaneously, resulting in extremely fast measurements.

The IR-beam is first sent through a beam splitter, where after one part of the beam is reflected on a stationary mirror where after it is sent through the sample to the detector. The other part of the beam is reflected of a movable mirror and then sent back through the sample to the detector, resulting in a difference in the length the light has to travel, controlled by the position of the movable mirror. The positive/destructive interference data from the interferometer is a graph of output light intensity versus retardation, retardation being the difference in path-length for the light hitting the movable mirror and hitting the stationary mirror [51].



### 3. Results and discussion

#### 3.1. Active phase characterization

As the Ag-alumina catalysts in Paper I-III was synthesized in-house the BET surface area was measured using nitrogen sorption [44] to verify a successful synthesis. The specific surface areas showed a high consistency for all samples and display a high surface area in the range 192 +/- 23 m<sup>2</sup>/g.

The state of the silver is thought to be of crucial importance in regards to the activity for NO<sub>x</sub> reduction. The Ag-alumina catalysts were investigated using both UV-vis spectroscopy (Paper I-II) as well as X-ray photoelectron spectroscopy (XPS) (Paper II) in order to retrieve information about the nature and distribution of the silver species. Previous UV-vis studies on Ag/Al<sub>2</sub>O<sub>3</sub> suggest that ionic silver species (Ag<sup>+</sup>) show absorption peaks in the range between 190 and 230 nm [52, 53]. Peaks at 290-350 nm are ascribed to small silver clusters between 2 and 7 atoms (Ag<sub>n</sub><sup>δ+</sup>), and peaks over 390 nm are suggested to derive from metallic silver (Ag<sup>0</sup>) [52, 53]. The UV-vis studies were performed on pure Ag-alumina samples, fresh and aged, as well as on Ag-alumina catalysts doped with 500 ppm of platinum. Sol-gel synthesized pure γ-alumina was used as reference and this spectrum was subtracted from the Ag-alumina data, resulting in a graph displaying the silver absorption intensity. The adsorption band of different silver species has been studied intensely, and the absorption spectra were deconvoluted as follows: silver ions (Ag<sup>+</sup>) P1=230 nm [52], silver clusters (Ag<sub>n</sub><sup>δ+</sup>) P2=300 nm and P3=360 nm [52], metallic silver (Ag<sup>0</sup>) ascribed to peaks above 390 nm, determined by best fit to 425 nm and 545 nm. The absorption spectrum for Ag6, from Paper II, with deconvolution peaks as well as the sum of the peaks, are show in Figure 2. The area of the specific peaks in relation to the total absorption gives the ratio of the different silver species. The results, shown in Table 1, indicate that the ratio between Ag<sup>+</sup>, Ag<sub>n</sub><sup>δ+</sup> and Ag<sup>0</sup> remain very similar as the silver loading is altered, also when the sample is doped with 500 ppm Pt (Paper II). The overall UV-vis absorption increases for the samples in the order Ag2 < Ag2Pt500 < Ag6 < Ag6Pt500. The peaks around 230 nm and 360 nm are clearly visible for all samples and the peak at 300 nm is visible for the 2 wt% Ag samples.

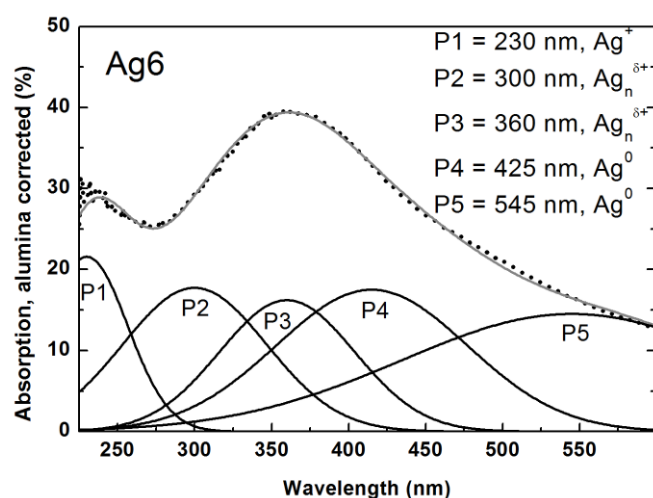


Figure 2: UV-vis spectrum (alumina spectra compensated) for Ag6 with total absorption (dotted line), deconvolution peaks (P1-P5) and the sum of the deconvolution peaks (solid line).

Table 1: Sample denotation, specific surface area (BET) and relative amount of  $\text{Ag}^+$ ,  $\text{Ag}_n^{\delta+}$  and  $\text{Ag}^0$  (UV-vis) of the  $\text{Ag}/\text{Al}_2\text{O}_3$  samples.

Sample composition	Sample designation	SSA <sup>a</sup> ( $\text{m}^2/\text{g}$ )	$\text{Ag}^{+,b}$ (%)	$\text{Ag}_n^{\delta+,c}$ (%)	$\text{Ag}^{0,d}$ (%)
2 wt% $\text{Ag}/\text{Al}_2\text{O}_3$	Ag2	189	11	38	51
2 wt% $\text{Ag}/\text{Al}_2\text{O}_3$ w. 500 ppm Pt	Ag2Pt500	215	14	39	47
6 wt% $\text{Ag}/\text{Al}_2\text{O}_3$	Ag6	167	17	37	46
6 wt% $\text{Ag}/\text{Al}_2\text{O}_3$ w. 500 ppm Pt	Ag6Pt500	182	17	37	46

<sup>a</sup> BET surface area. <sup>b</sup>  $\text{Ag}^+$  ionic silver, P1 at 230 nm [52]. <sup>c</sup>  $\text{Ag}_n^{\delta+}$  silver clusters P2=300 nm and P3=360 nm [52]. <sup>d</sup>  $\text{Ag}^0$  metallic silver P4=415 nm and P5=545 nm.

The UV-vis data indicate that the ratio between ionic silver species, small silver clusters and metallic silver particles is similar for the Ag2, AgPt500, Ag6 and Ag6Pt500 samples. Although the ratios remain similar despite the difference in silver loading, a slight increase of the ionic species, on the expense of the metallic ones, is observed as the silver loading is increased (Table 1). Platinum doping appears to alter the ratios slightly for the 2 wt% Ag sample with a small increase of the ionic species for the platinum containing sample, but no change is observed when adding platinum to the Ag6 sample. This may owe to the abundance of silver in the latter case, overpowering the effects of the platinum. Furthermore, no additional UV-vis peaks can be observed for the Pt-doped samples. However, at these low platinum levels, absorption peaks for Pt should be very hard to detect. The overall UV-vis results indicate that no significant difference can be seen between the four samples.

In addition to the UV-vis spectroscopy, the samples were investigated using XPS. The binding energy for the  $\text{Ag } 3d_{5/2}$  peak and the distance between the  $\text{Ag } 3d_{5/2}$  and the  $\text{Ag } 3d_{3/2}$  peaks were investigated for the Ag2, Ag2Pt500, Ag6 and Ag6Pt500 samples, as well as for fresh and aged 2 and 6 wt% samples. The results from pure and Pt doped samples show that the  $\text{Ag}3d_{5/2}$  peak is centralized around 367.7 eV, similar to results by Bukhtiyarov *et al.*, validating the existence of  $\text{Ag}^+$  species [54], with a peak to peak distance between 5.9 and 6.2, in accordance with literature data [55]. The binding energy for  $\text{Ag}3d_{5/2}$  and the peak distance between the  $\text{Ag}3d_{5/2}$  and the  $\text{Ag}3d_{3/2}$ , are shown in Table 2. The results further indicate that the ratio between different silver species does not change with silver loading and/or Pt-doping. The measurements on the fresh and aged 2 and 6 wt% samples show a slight shift with 0.3 eV up to 367.9 eV with a slight change for the 2 wt% sample of 0.4 eV between the fresh and aged samples, however no change was observed for the 6 wt% sample. This indicates that the aging does not influence the nature of the silver to any significant degree.

Table 2: Binding energy for the  $\text{Ag}3d_{5/2}$  peak and the distance between the  $\text{Ag}3d_{5/2}$  and the  $\text{Ag}3d_{3/2}$  peaks for fresh and aged 2 and 6 wt%  $\text{Ag}/\text{Al}_2\text{O}_3$  samples (Paper I) as well as 2 wt%  $\text{Ag}/\text{Al}_2\text{O}_3$ , 2 wt%  $\text{Ag}/\text{Al}_2\text{O}_3$  with 500 ppm platinum, 6 wt%  $\text{Ag}/\text{Al}_2\text{O}_3$ , 6 wt%  $\text{Ag}/\text{Al}_2\text{O}_3$  with 500 ppm platinum (Paper II).

	Ag2 fresh	Ag2 aged	Ag6 fresh	Ag6 aged	Ag2 fresh	Ag2Pt500 fresh	Ag6 fresh	Ag6Pt500 fresh
BE (eV)	367.5	367.9	367.9	367.9	367.6	367.7	367.7	367.7
$\Delta\text{BE}$ (eV)	6.1	6.1	6.1	6.2	5.9	5.9	6.0	5.9

### 3.2. Hydrocarbon oxidation

One of the most important steps in the lean reduction of  $\text{NO}_x$  via hydrocarbons is the accessibility of the hydrocarbon, *e.g.* the amount and reactivity of surface HC and its reactivity. The amount of HC surface species has been found to depend on the type of hydrocarbon, surface properties as well as temperature. The effect of different reducing agents and surface properties were investigated in Paper I using a representative hydrocarbon for gasoline, n-octane, and a commercial bio-diesel, NExBTL, while changing the silver loading. The influence of Ag-loading and type of reducing agent on the hydrocarbon conversion is shown in Figure 3. In general, when comparing n-octane to NExBTL, the hydrocarbon conversion can be seen to be higher for n-octane at lower temperatures while the conversion of NExBTL is higher at high temperatures. The difference in high temperature conversion for the Ag2 sample can be seen to owe to a leveling out of the n-octane conversion *cf.* NExBTL. Although the formation of CO does not vary significantly between the different samples, reaching a maximum of 200 ppm, the  $\text{CO}_2$  formation produced either from the combustion reaction or the  $\text{NO}_x$  reduction reaction, varies to a larger degree.

As stated previously, NExBTL consists mainly of iso-paraffins [53] and have an approximate carbon chain-length of 16 compared to n-octane. This difference will most likely influence the adsorption behavior of the hydrocarbons, and the high amount of branching in the NExBTL can lead to increased adsorption as compared to the n-octane. This is in accordance to results from Lindfors *et al.* [56], where branched hydrocarbons display a lower activity compared to straight hydrocarbons. The Ag6 sample does, however, have higher number of oxidation sites than the 2 wt% sample and can thus oxidize the adsorbed hydrocarbon to a higher degree, facilitating a slightly higher HC conversion. A sharp increase in HC conversion can be seen above 300°C. As the temperature increases above 300°C, silver

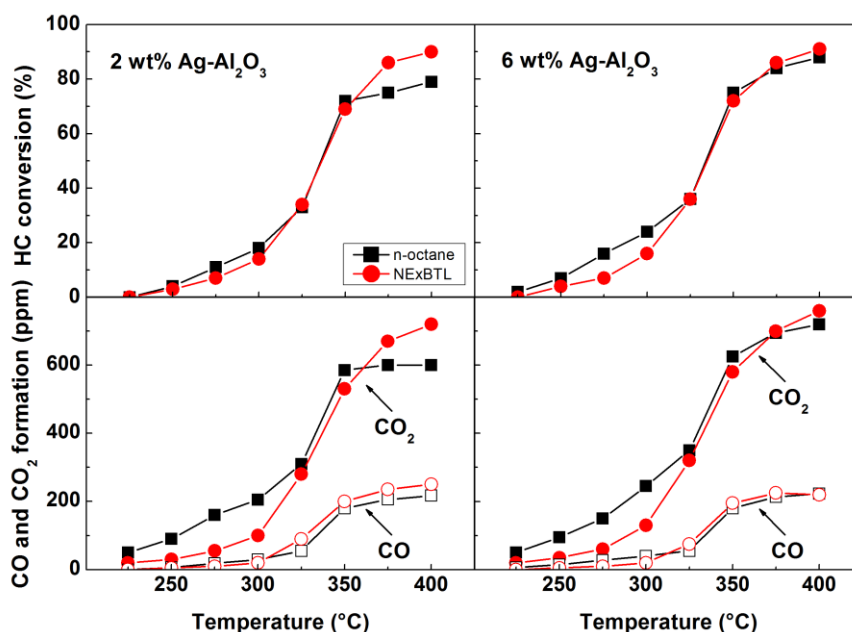


Figure 3: The hydrocarbon conversion and the CO and  $\text{CO}_2$  formation over temperature for the Ag2 and Ag6 samples during  $\text{NO}_x$  reduction experiments, using n-octane and NExBTL as reducing agents. Inlet gas composition: 200 ppm  $\text{NO}$ , 10 %  $\text{O}_2$ , 1000 ppm  $\text{H}_2$ , 5 %  $\text{H}_2\text{O}$ ,  $\text{Ar}_{\text{bal}}$  and n-octane or NExBTL as reducing agent with a C/N molar ratio of 6. GHSV = 33, 200  $\text{h}^{-1}$ .

most likely is reduced from a surface oxide to metallic silver [57], increasing the oxidative properties and improving the HC oxidation activity. This would also explain why the experiment performed with NExBTL show a higher HC-conversion and CO<sub>2</sub> formation at high temperatures, as compared to the n-octane. In addition, the length and branching of the hydrocarbon chain likely influence the type of oxygenated hydrocarbon species formed on the surface [56]. Hence, the surface coverage of NExBTL and/or NExBTL derived species would likely be higher in comparison with the case of n-octane, effectively poisoning the surface.

To further investigate the relation between the nature of the hydrocarbon and its ability to be oxidized, hydrocarbons with different carbon-carbon bond order (i.e., alkane, alkene, and alkyne), were investigated in Paper III. The results show the formation of CO and CO<sub>2</sub> when these hydrocarbons are oxidized with O<sub>2</sub> over Ag<sub>2</sub> and Ag<sub>6</sub> catalysts during extinction (cooling) ramp experiments (Figure 4). In general the hydrocarbon oxidation proceeds at lower temperatures and results in higher CO<sub>2</sub> formation over the Ag<sub>6</sub> sample as compared to the Ag<sub>2</sub> sample. This is particularly evident in the case of C<sub>2</sub>H<sub>4</sub> oxidation, which starts around 350°C over the Ag<sub>6</sub> sample but not below 450°C over the Ag<sub>2</sub> sample. For both catalysts, the lowest activation temperature is observed for ethyne (C<sub>2</sub>H<sub>2</sub>) oxidation, which starts around 270 and 300 °C for the Ag<sub>6</sub> and Ag<sub>2</sub> samples, respectively. The formation of CO and CO<sub>2</sub> is also significantly higher during oxidation of C<sub>2</sub>H<sub>2</sub> as compared to the other hydrocarbons. The highest temperature for oxidation onset is observed for C<sub>2</sub>H<sub>6</sub>, and the oxidation pattern is generally similar for both catalysts although the CO<sub>2</sub>/CO ratio is slightly higher over the Ag<sub>6</sub> sample. The activation temperature for oxidation of all hydrocarbons is lower over the Ag<sub>6</sub>

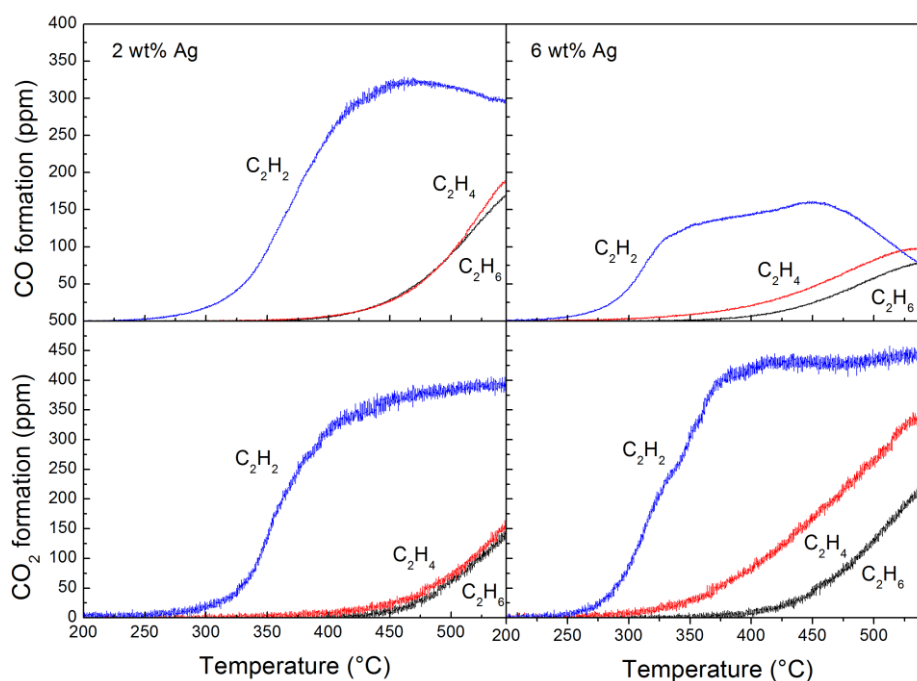


Figure 4: Formation of CO and CO<sub>2</sub> during temperature programmed extinction experiments with C<sub>2</sub>H<sub>2</sub> (blue), C<sub>2</sub>H<sub>4</sub> (red), and C<sub>2</sub>H<sub>6</sub> (black) over Ag<sub>2</sub> and Ag<sub>6</sub> catalyst. Inlet gas composition: 600 ppm C<sub>2</sub> hydrocarbon, 10% O<sub>2</sub>, Ar<sub>bal.</sub> GHSV: 32,000 h<sup>-1</sup>.

sample, while the CO formation is higher for the Ag2 sample. This is probably connected to the presence of a higher amount of metallic silver species in the Ag6 catalyst compared to the Ag2 catalyst, facilitating total oxidation in agreement with previous studies [32, 58]. This is further supported by the lower CO and higher CO<sub>2</sub> concentrations observed for the Ag6 catalyst, compared to the Ag2 catalyst. To understand the underlying reasons for the increased oxidation for C<sub>2</sub>H<sub>4</sub> and C<sub>2</sub>H<sub>6</sub> many aspects need to be taken into consideration. Steric effects resulting in differences in the hydrocarbon activation/oxidation have been discussed for C–H bond interaction with the catalyst surface. For instance Siegbahn [59] investigated the relation between hydrocarbon activation and C–H bond strength for ethyne, ethene, and methane and found that for second row transition metals acting as catalyst this relation is inverse. Even though ethyne possesses the strongest C–H bond among these hydrocarbons, the activation barrier for breakage of this bond is the lowest. This is explained by a steric effect, where C–H activation requires the metal, second row transition metal in this case, to interact more efficiently in a side way orientation with the C–H bond, which is facilitated for the straight ethyne molecule [59]. However, in the present case the C–C bond activation is likely more important than the activation of the C–H bond, not necessarily breaking the C–C bond but activating the molecule towards further reactions. The adsorption of the hydrocarbon is also dependent of the shape and orientation of the C–C electron orbitals. The electrons in the  $\pi$ -bonds in ethene and especially ethyne, for which the  $\pi$ -electron cloud has a cylindrical shape, can easily interact with the catalyst surface and thereby form new bonds between the unsaturated hydrocarbon and the surface. Furthermore, the difference in steric hindrance is to a high extent reflected in the sticking probability. As comparative studies on the sticking probabilities of C<sub>2</sub> hydrocarbons on silver are rare, we here attempt to discuss this matter generally, based on observations for other systems. It has, for instance, been shown that the sticking probability for C<sub>2</sub> (C<sub>2</sub>H<sub>x</sub>, x = 0–6) hydrocarbons on diamond (111) generally decreases as the number of hydrogen atoms in the molecule increases [60]. This is caused by an increased reflection of the approaching molecule by shielding because of the higher number of hydrogen atoms.

As stated above, the surface properties of the catalyst are of high importance when studying oxidation properties. To further understand the oxidation of the hydrocarbon over the Ag-alumina surface, separate hydrocarbon oxidation experiments were performed using n-octane, also including Ag-alumina samples doped with platinum (Paper II). When comparing hydrocarbon oxidation results for the Pt-doped and pure Ag catalysts (Figure 5) it can be seen that the HC conversion for the Pt-doped samples starts at much lower temperatures. For instance, the HC conversion for the Ag2Pt500 sample starts already at 250°C, which should be compared to well above 300°C for the corresponding, un-doped Ag sample, similar to the steep increase in the HC-oxidation for n-octane and NExBTL during NO<sub>x</sub> reduction experiments

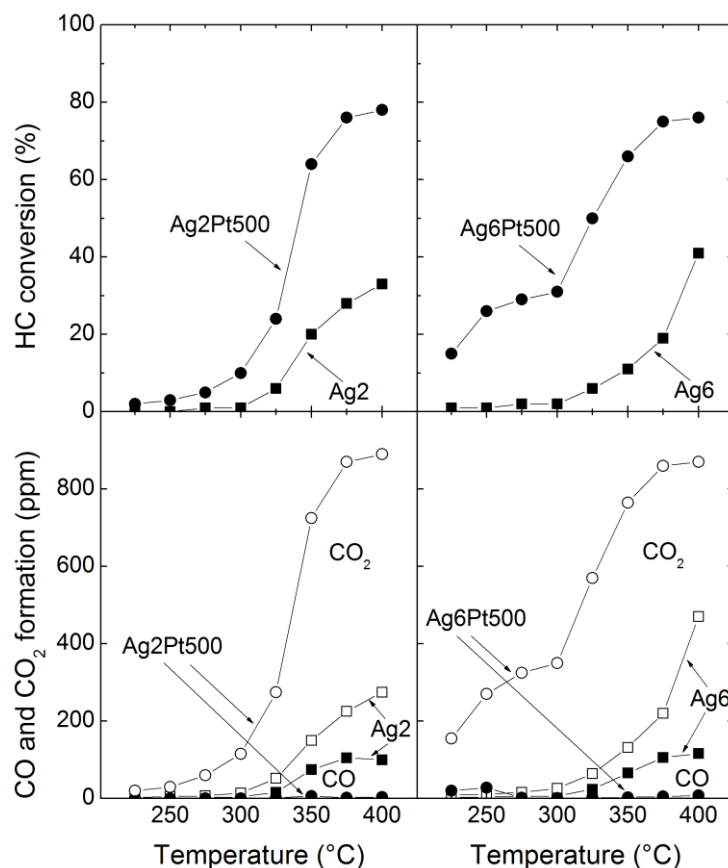


Figure 5: HC oxidation for the Ag<sub>2</sub>, Ag<sub>2</sub>Pt<sub>500</sub>, Ag<sub>6</sub> and Ag<sub>6</sub>Pt<sub>500</sub> samples. Top: HC conversion. Bottom: CO and CO<sub>2</sub> formation. Inlet gas composition: 150 ppm n-octane, 1000 ppm H<sub>2</sub>, 5 % H<sub>2</sub>O, 10 % O<sub>2</sub> with Ar<sub>bal</sub>. GHSV = 33, 200 h<sup>-1</sup>.

using pure Ag-alumina catalysts. The HC conversion for the Ag<sub>6</sub>Pt<sub>500</sub> sample starts before 225°C, however the conversion increase drops at 325°C, similar to the drop in NO<sub>x</sub> reduction activity, see 4.3. Generally, the silver species most likely attain a more metallic structure as the temperature is increased (>300°C), as stated before [57], which likely results in an adsorption/oxidation equilibrium balance, where the rate of oxidation is similar the rate of adsorption. Hence, the surface converge of hydrocarbons decreases and other species, *i.e.* NO<sub>x</sub>, can adsorb and react. Moreover, the UV-vis and XPS results indicate that increasing the silver loading leads to an increase in the total number of oxidation sites (the ratios being constant), which results in an increase in HC oxidation at high temperature, for the high-loaded Ag samples. The increased hydrocarbon oxidation at low temperatures, for the Pt-doped samples can, on the other hand, likely derive from an increased adsorption energy of the hydrocarbon on the surface. Comparing the dissociation energies for different molecules on silver and platinum surfaces, the dissociation energy is always lower for platinum according to Bligaard *et al.* [61]. The authors report that the dissociative chemisorption for CH<sub>4</sub> on platinum cf. silver differs by 6.49 eV [61]. The Brøsted-Evans-Polansky (BEP) relation [62, 63] states that the change in activation energy follows the change in energy of the final state for the chemically dissociated molecule. Although the difference likely is smaller for higher hydrocarbons, the sticking probability on platinum is still prone to be higher than on silver. Although the metals in the present samples may be more or less oxidized, the BEP relation holds also for oxides

[64] which ensures that the activation barrier will be lower for the oxidized particles as well. Thus, the relative sticking probability should be higher over Pt species than over corresponding Ag species. Furthermore, assuming that incorporation of platinum increases the adsorption of hydrocarbons, the Ag<sub>2</sub>Pt500 sample should be more susceptible to hydrocarbon poisoning compared to the Ag<sub>6</sub>Pt500 sample, due to its lower number of oxidation sites. The Ag<sub>6</sub>Pt500 sample will instead reach adsorption/oxidation equilibrium at lower temperatures and hence have a higher overall HC conversion and a higher HC conversion at lower temperatures. Previous studies have suggested that the activity for NO<sub>x</sub> reduction over Ag-alumina is affected by many parameters, such as the ratio between oxidation and reduction sites [32], the dissociative chemisorption of hydrocarbons [65, 66] and, in relation to this, the influence of C-C bond strength, steric effects and sticking probability, i.e. hydrocarbon-surface interaction [34]. The effect of the platinum addition to the silver-alumina system could possibly be ascribed to all of these parameters. Pt may change the amount of chemisorbed hydrocarbon on the surface and thereby possibly change the required ratio of red/ox sites for efficient partial oxidation of the hydrocarbon. It may also alter the effective oxidation properties of the surface.

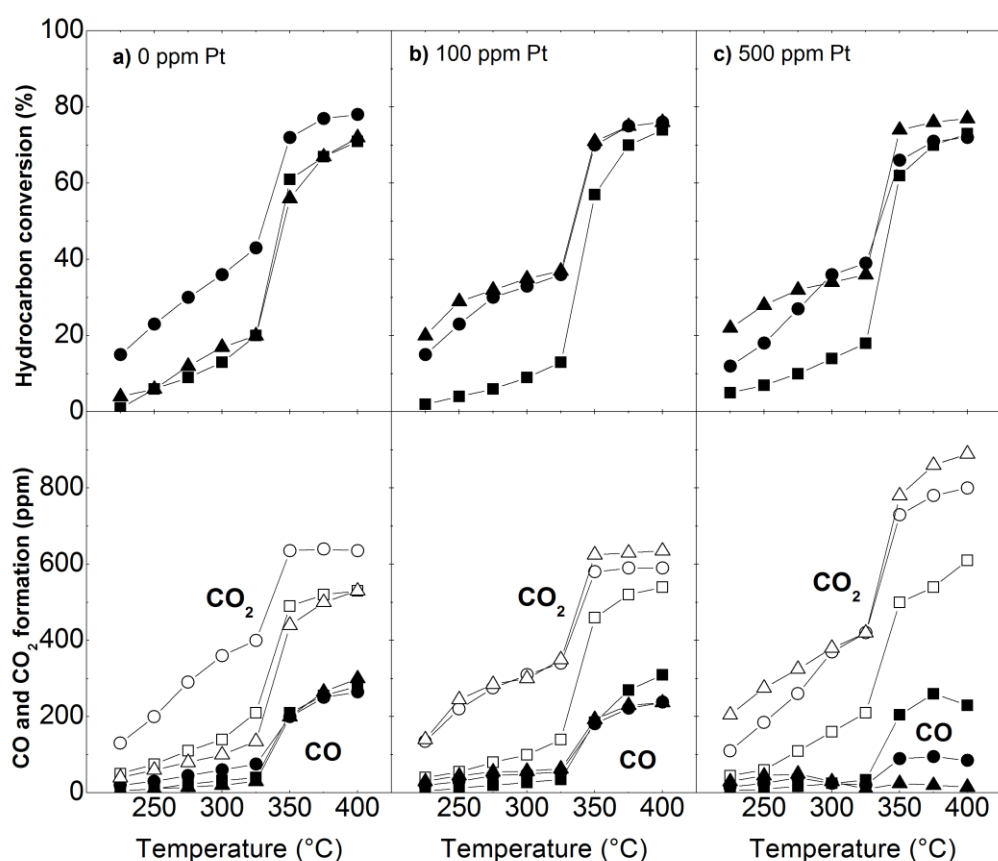


Figure 6: Hydrocarbon conversion (top) as well as CO and CO<sub>2</sub> formation (bottom) from NO<sub>x</sub> reduction experiments in flow reactor for 2 wt% (■), 4 wt% (●) and 6 wt% (▲) Ag/Al<sub>2</sub>O<sub>3</sub> samples without Pt (left column), with 100 ppm Pt (center column) and with 500 ppm Pt (right column). Inlet gas composition: 200 ppm NO, 10 % O<sub>2</sub>, 1000 ppm H<sub>2</sub>, 5 % H<sub>2</sub>O, Ar<sub>bal</sub> and n-octane as reducing agent with a C/N molar ratio of 6. GHSV = 33, 200 h<sup>-1</sup>.

Comparing the hydrocarbon conversions for the Ag2 and Ag6 samples in Figure 5 and 5, a higher HC conversion can be seen from the NO<sub>x</sub> reduction experiments. The conversion for the Pt-doped samples, Ag2Pt500 and Ag6Pt500, is seen to differ less, however the low temperature HC conversion is higher for the NO<sub>x</sub> reduction experiments. The higher HC conversion at low temperature is likely owing to the presence of reactive nitrite species. As the HC conversion is calculated from the CO and CO<sub>2</sub> formation (Eq. 3 and 4), the difference in HC conversion could also be ascribed to the formation of other partially oxidized carbon containing species during the HC oxidation experiments, such as *e.g.* acetates.

### 3.3. NO<sub>x</sub> reduction activity

The influence of Ag-loading and type of reducing agent on the lean NO<sub>x</sub> reduction performance, for fresh samples and for samples hydrothermally (HT) treated at 500°C, 10% H<sub>2</sub>O and 10% O<sub>2</sub> with argon balance for 12 hours, is illustrated in Figure 7 (Paper I). In general, the hydrothermal treatment results in a slight increase in the lean NO<sub>x</sub> reduction. Furthermore, a higher silver loading results in an increased activity for NO<sub>x</sub> reduction, both for n-octane and NExBTL as reductant. It can also be observed that the activity for NO<sub>x</sub> reduction is lower when using NExBTL as reducing agent, compared to n-octane.

For n-octane as reducing agent the fresh 2 wt% Ag sample displays somewhat higher NO<sub>x</sub> reduction, as compared to the HT-treated sample, at temperatures between 225 and 325°C. The Ag6 sample shows similar NO<sub>x</sub> reduction below 300°C for both the fresh and the HT-treated sample. Above 350°C, the HT-treatment results in a slight increase of approximately 5% in the NO<sub>x</sub> reduction over both catalysts, reaching a maximum of 66% at 350°C for Ag2 sample and a maximum of 78% at 375°C for the Ag6 sample.

For NExBTL as reducing agent, similar trends as for n-octane are observed, however the NO<sub>x</sub> reduction starts at higher temperatures. For the HT-treated 2 wt% Ag sample, a slight increase in NO<sub>x</sub> reduction is observed above 300°C, as compared to the fresh sample, although no significant differences are observed at lower temperatures. The 6 wt% Ag sample shows similar activity for NO<sub>x</sub> reduction, both when fresh and HT-treated. Both samples display high activity for lean NO<sub>x</sub> reduction, reaching a maximum of 50 and 60% at 375°C for the 2 and 6 wt% Ag sample, respectively. The activity for NO<sub>x</sub> reduction can be seen to increase with increasing n-octane conversion (Figure 3), when the silver loading is increased from 2 to 6 wt%, as seen in Figure 7. It is interesting to note, however, that the increase in NO<sub>x</sub> reduction is higher than the corresponding increase in HC conversion, indicating that a higher Ag loading results in a more effective usage of the hydrocarbon in the selective NO<sub>x</sub> reduction reaction. The difference between NO<sub>x</sub> reduction and HC conversion is less pronounced when using NExBTL as reductant. Furthermore, the NExBTL conversion over the 6 wt% Ag sample decreases after the HT-treatment, indicating a higher NO<sub>x</sub> reduction efficiency.

The effect of ageing at higher temperatures was also investigated, see Paper I. It can be seen that ageing at temperatures up to 650°C is beneficial towards the NO<sub>x</sub> reduction, with an increase in activity of up to 15%. However, when the ageing temperature exceeds 650°C the activity decreases severely. Furthermore, the maximum activity is located around 350°C for the fresh samples and the samples aged between 500 and 650°C, while this maximum shifts towards higher temperatures for samples aged at 700°C and above.

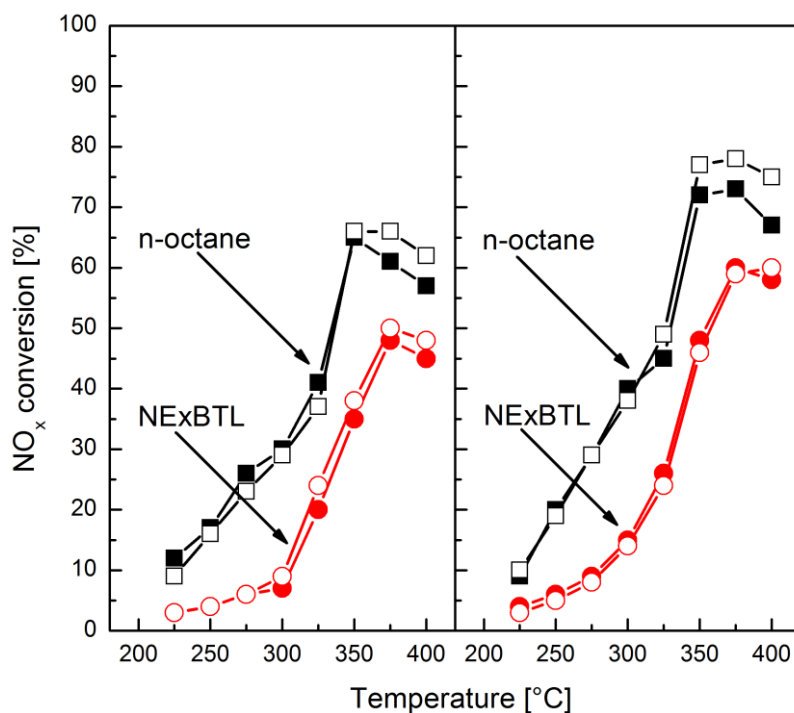


Figure 7:  $\text{NO}_x$  reduction from flow reactor experiments for fresh (closed markers) and hydrothermally treated (open markers) 2 and 6 wt%  $\text{Ag}/\text{Al}_2\text{O}_3$  using n-octane (■, □) or NExBTL (●, ○) as reducing agent. Inlet gas composition: 200 ppm  $\text{NO}$ , 10 %  $\text{O}_2$ , 1000 ppm  $\text{H}_2$ , 5 %  $\text{H}_2\text{O}$  and  $\text{Ar}_{\text{bal}}$ ,  $\text{C}/\text{N}=6$ .  $\text{GHSV} = 33, 200 \text{ h}^{-1}$

As discussed in section 3.2, the structure of the NExBTL, with its high degree of branching, will likely lead to increased surface coverage of NExBTL and/or NExBTL-derived species, as compared to the case of n-octane. This will likely lead to partial poisoning, reducing the amount of nitrogen-containing species on the surface. This is thought to be the reason for the lowered  $\text{NO}_x$  reduction activity when changing from n-octane to NExBTL.

The addition of platinum to the silver-alumina showed to significantly alter the hydrocarbon oxidation properties of the catalyst (Figure 5). The effect of platinum is also very visible on the  $\text{NO}_x$  reduction ability. The activity for  $\text{NO}_x$  reduction under lean conditions, for the 2, 4 and 6 wt% silver alumina samples, pure and doped with 100 or 500 ppm of platinum are shown in Figure 8. The activity for  $\text{NO}_x$  reduction for the samples without Pt doping follow a typical volcano shape, with an increased activity with higher temperature up to around  $350^\circ\text{C}$ , after which the competing combustion reaction becomes dominant and the  $\text{NO}_x$  reduction decreases. The Ag2 and Ag4 samples show similar performance for  $\text{NO}_x$  reduction up to  $325^\circ\text{C}$ . At higher temperatures however, the Ag2 sample show higher  $\text{NO}_x$  reduction. The Ag6 sample show slightly lower  $\text{NO}_x$  reduction below  $325^\circ\text{C}$ , compared with the Ag2 and Ag4 samples, but displays the highest  $\text{NO}_x$  reduction above  $350^\circ\text{C}$ .

Introducing Pt to the samples generally improves the low-temperature activity for lean  $\text{NO}_x$  reduction. However, although the activity for  $\text{NO}_x$  reduction over the Ag2Pt100 sample resembles that of the pure  $\text{Ag}/\text{Al}_2\text{O}_3$  samples, increasing the silver loading further results in lowered activity for  $\text{NO}_x$  reduction, reaching a minimum around  $325^\circ\text{C}$  for the Ag4Pr100 and Ag6Pt100 samples. The  $\text{NO}_x$  reduction for these samples increases again as the temperature reaches  $350^\circ\text{C}$  although the activity does not reach that of the pure  $\text{Ag}/\text{Al}_2\text{O}_3$  samples. The

Ag2Pt100 sample shows the highest activity for NO<sub>x</sub> reduction above 350°C. The results from the samples doped with 500 ppm Pt show an even higher activity at low temperatures, with the highest activity for the Ag2Pt500 sample. The decrease in activity, localized around 325°C, is however observed for all Pt doped samples, regardless of silver loading. The decrease becomes more prominent and starts at lower temperatures as the silver loading is increased.

The outlet concentrations of NO and NO<sub>2</sub> indicate that the ratio between NO and NO<sub>2</sub> is quite similar for the pure silver alumina samples with NO as the dominant NO<sub>x</sub> species over the entire temperature range. For the samples doped with 100 ppm Pt, the NO/NO<sub>2</sub> ratio is altered, showing a higher NO<sub>2</sub> concentration at low temperatures. At high temperatures NO is again the dominating gas phase NO<sub>x</sub> species. The NO and NO<sub>2</sub> concentrations are similar for the Ag2Pt100 and Ag4Pt100 samples, whereas the NO<sub>2</sub> concentration is substantially higher for the Ag6Pt100 sample. Further, for the samples doped with 500 ppm Pt, the Ag2Pt500 sample shows a similar trend as the Ag2 sample, with a high NO concentration observed at low temperatures. The Ag4Pt500 and the Ag6Pt500 samples show similar trends as the corresponding samples doped with 100 ppm Pt, showing low NO concentrations at low temperatures. The NO<sub>2</sub> concentration follows the opposite trend with high concentrations at low temperatures, decreasing with increasing temperature. Previous studies [67] have shown that varying the inlet NO/NO<sub>2</sub>-ratio generally have a negligible influence on the overall NO<sub>x</sub> reduction, and that that the effect of introducing NO<sub>2</sub> in the feed even is negative for the overall reduction of NO<sub>x</sub> when using n-octane as reducing agent [67]. Meunier *et al.* [68] found a promotional effect when using NO<sub>2</sub> as reactant, however these experiments were performed with low oxygen concentrations using C<sub>3</sub>H<sub>8</sub> as reducing agent. During such conditions, a strong oxidizing agent as NO<sub>2</sub> might be beneficial.

The overall results show that, as the catalysts are doped with platinum, the oxidation of NO to NO<sub>2</sub> is changed, but as stated before this is not thought to play a major role in the NO<sub>x</sub> reduction reaction under the present reaction conditions. No clear trend from the NO oxidation experiments or the NO/NO<sub>2</sub> concentration during the NO<sub>x</sub> reduction experiments is found which can explain the change in NO<sub>x</sub> reduction activity observed for the platinum-doped samples. However, the HC oxidation experiments show that the addition of platinum alters the HC oxidation properties for the Ag-alumina catalysts, resulting in two oxidation regimes. This double regime behavior, with a minimum HC conversion at 325°C, is related to the NO<sub>x</sub> reduction activity also showing two conversion regimes. As the temperature increases, the amount of available hydrocarbon on the surface increases, possibly owing to that the inactive nitrates desorb allowing more hydrocarbons to adsorb on the surface. For the high-loaded samples with 500 ppm platinum the amount of hydrocarbon starts to poison the surface and the NO<sub>x</sub> reduction activity starts to decrease. As the temperature reaches 325°C, the hydrocarbon oxidation over the pure silver sites starts and the excess hydrocarbon is purged from the surface, resulting in a decrease in activity with a minimum around 325°C, which is then recovered to a certain degree. Hence, the change in HC oxidation performance and the increase in hydrocarbon adsorption on the surface are suggested to be the underlying reason for the two reduction regimes for NO<sub>x</sub>. This effect leads us to suggest that, although the NO to NO<sub>2</sub> formation likely is of some importance, it is the increase in sticking probability and partial oxidation of the hydrocarbon, owing to the added platinum, that is the main factor leading

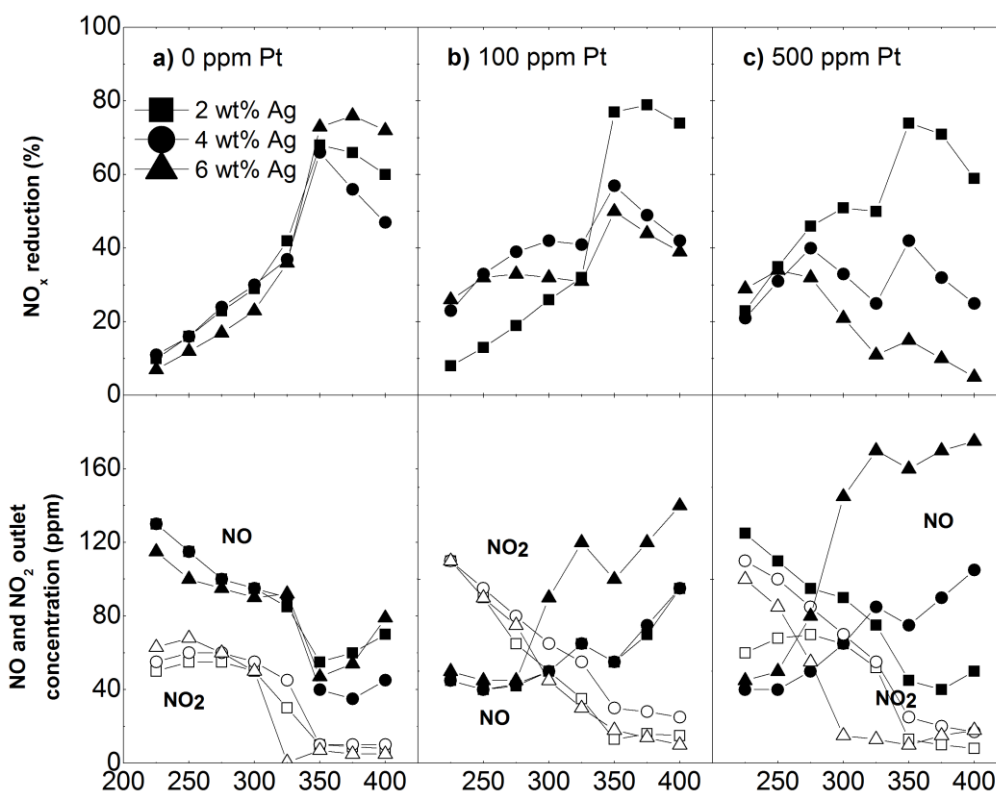


Figure 8: NO<sub>x</sub> reduction (top) as well as outlet concentration of NO and NO<sub>2</sub> (bottom) from NO<sub>x</sub> reduction experiments in flow reactor for 2 wt% (■), 4 wt% (●) and 6 wt% (▲) Ag/Al<sub>2</sub>O<sub>3</sub> samples without Pt (left column), with 100 ppm Pt (center column) and with 500 ppm Pt (right column). Inlet gas composition: 200 ppm NO, 10 % O<sub>2</sub>, 1000 ppm H<sub>2</sub>, 5 % H<sub>2</sub>O, Ar<sub>bal</sub> and n-octane as reducing agent with a C/N molar ratio of 6. GHSV = 33, 200 h<sup>-1</sup>.

to the increase in NO<sub>x</sub> reduction at low temperatures for the Pt-doped samples. This implies that the doped samples have more available hydrocarbon on the surface, owing to higher sticking probability, and the increase in low-temperature NO<sub>x</sub> reduction is actually a result of this effect.

Figure 9 shows the NO<sub>x</sub> reduction and CO and CO<sub>2</sub> formation during oxidation of C<sub>2</sub> hydrocarbons in the presence of NO and excess O<sub>2</sub> over the Ag<sub>2</sub> and Ag<sub>6</sub> samples during extinction ramp experiments. The NO<sub>x</sub> reduction pattern is in general similar for both catalysts although the temperature windows are shifted to lower temperatures and the maximum NO<sub>x</sub> reduction is slightly lower for the Ag<sub>6</sub> sample. The highest NO<sub>x</sub> reduction is achieved when C<sub>2</sub>H<sub>2</sub> is used as reducing agent, over both catalysts, reaching 87% at 427 °C for the Ag<sub>2</sub> sample. For both catalysts the C<sub>2</sub>H<sub>2</sub> also shows the widest temperature window for NO<sub>x</sub> reduction. The maximum NO<sub>x</sub> reduction for C<sub>2</sub>H<sub>4</sub> and C<sub>2</sub>H<sub>6</sub> is 71 and 81%, respectively, over the Ag<sub>2</sub> sample and around 70% over the Ag<sub>6</sub> sample. The temperature windows for NO<sub>x</sub> reduction with these hydrocarbons are similar, showing no significant activity below 350 and 400°C for the Ag<sub>6</sub> and Ag<sub>2</sub> samples, respectively. The hydrocarbon oxidation profile in the presence of NO is similar for both catalysts, however, significantly different compared to oxidation in absence of NO.

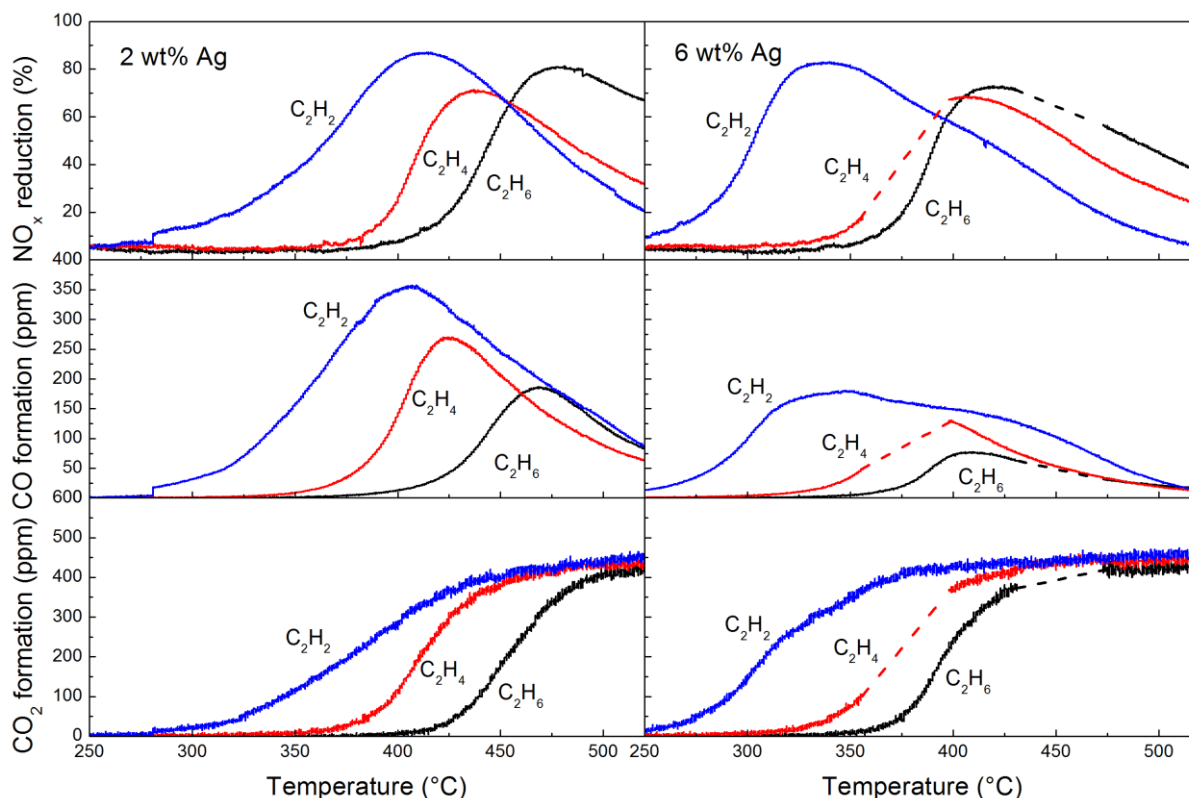


Figure 9: Formation of CO, CO<sub>2</sub> and reduction of NO<sub>x</sub> during temperature programmed extinction experiments with C<sub>2</sub>H<sub>2</sub> (blue), C<sub>2</sub>H<sub>4</sub> (red), and C<sub>2</sub>H<sub>6</sub> (black) over Ag/Al<sub>2</sub>O<sub>3</sub> catalyst with (a) 6 wt % and (b) 2 wt % nominal silver content. Inlet gas composition: 200 ppm NO, 600 ppm C<sub>2</sub>hydrocarbon, 10% O<sub>2</sub>, Ar<sub>bal</sub>. GHSV: 32,000 h<sup>-1</sup>.

The silver loading can be seen to significantly influence both the NO<sub>x</sub> reduction activity as well as the temperature for maximum reduction, independent of reducing agent (Paper I -III). As the ratio between the surface silver species is constant for the different silver loadings (Paper II), the number of active sites probably plays a major role. A higher number of sites would decrease the distance between the different sites, likely increasing the interaction between the oxidative and reductive sites. Paper II-III also illustrates the importance of the nature of the reducing agent with emphasis on carbon-carbon bond order, hydrocarbon branching and surface sticking probability.

## 4. Conclusions

This licentiate study shows a high catalytic activity for lean NO<sub>x</sub> reduction over the silver alumina catalyst for model hydrocarbons and for a commercial bio-diesel as the reducing agent for NO<sub>x</sub> (Paper I-II). The results show that silver-alumina catalysts, prepared via sol-gel synthesis, display a high consistency regarding surface area, and nature and relative amount of surface silver species, as the silver loading is varied. The samples also display a high tolerance towards hydrothermal ageing (Paper I-II). Furthermore, it can be concluded that as the samples are doped with trace-amounts of platinum, the activity for lean NO<sub>x</sub> reduction at low temperatures increases. It is additionally shown that both the silver loading and the type of reducing agent have a crucial effect on the catalytic performance. The catalyst composition with the highest activity for NO<sub>x</sub> reduction is found to be a 2 wt% loaded Ag/Al<sub>2</sub>O<sub>3</sub> sample doped with 500 ppm platinum when using n-octane as reducing agent (Paper II). This catalyst displays the highest low-temperature activity, which is most likely owing to an increased amount of partially oxidized hydrocarbon on the surface as well as a change in the oxidation potential attributed to the Pt doping. A higher hydrocarbon adsorption could mean that a lower amount of reducing agent would be required for Pt-doped silver-alumina catalysts as compared to the corresponding un-doped samples, improving fuel efficiency.

For n-octane, the silver-alumina samples display higher NO<sub>x</sub> reduction after ageing up to 650°C, compared to fresh samples, whilst the activity for lean NO<sub>x</sub> reduction decreases after ageing at 700°C and above. A higher silver loading results in a higher NO<sub>x</sub> reduction and a more efficient use of the reducing agent. Additionally it is shown that the catalytic performance of the silver-alumina sample is stable when subjected to mild hydrothermal treatment (500°C), which further enhances the efficiency of the reducing agent.

A systematic study of the influence of carbon-carbon bond order (C<sub>2</sub>H<sub>2</sub>, C<sub>2</sub>H<sub>4</sub>, and C<sub>2</sub>H<sub>6</sub>) and silver loading (2 and 6 wt%) on the formation of partial oxidation products and lean NO<sub>x</sub> reduction performance over silver-alumina catalysts is presented. Flow reactor experiments show that the highest activity for hydrocarbon oxidation and lean NO<sub>x</sub> reduction is achieved when C<sub>2</sub>H<sub>2</sub> is oxidized in the presence of NO. This is in accordance with the stronger interaction between ethyne and the metal surface, owing to the easily accessible π-electrons, a favorable molecular orientation, and higher sticking probability for C<sub>2</sub>H<sub>2</sub> compared to the other C<sub>2</sub> hydrocarbons. For the studied hydrocarbons, the temperature window for NO<sub>x</sub> reduction is broadened and shifted towards lower temperatures as the C-C bond order increases. Increasing the silver loading from 2 to 6 wt% is favorable for the oxidizing reactions, leading to activation of both hydrocarbons and NO<sub>x</sub> at lower temperatures.

In conclusion, silver-alumina catalyst prepared via the sol-gel method show high activity for NO<sub>x</sub> reduction at low temperatures, with high resistance towards hydrothermal ageing. The addition of platinum can be seen to increase the activity for NO<sub>x</sub> reduction at low temperature. The catalysts are also shown to be compatible with renewable fuels, although the activity for NO<sub>x</sub> reduction is lower. Knowledge of the catalytic process, like the activation of the reducing agent and the NO<sub>x</sub> related chemistry, is of major importance for catalyst development. Detailed understanding of these processes will likely result in the possibility to tailor catalysts *e.g.* for future fuels.



## **5. Outlook**

These results indicate that the type of reducing agent is of crucial importance and this relation will be investigated further, expanding the use of bio fuels to ethanol fuels. This will be done in collaboration with the Oakridge National Laboratory, Tennessee, USA.

The study has also involved the usage of NExBTL and this work will continue together with Volvo ATR and the Royal Institute of Technology in Sweden, integrating fuel-reforming with HC-SCR, during real engine exhaust experiments. The goal is to supply the needed hydrogen from the fuel-reformer and deliver proof of concept results from engine bench tests.

Future studies will also include impregnated Ag/Al<sub>2</sub>O<sub>3</sub> with or without platinum doping, with the goal of distinguishing between the cluster size importance, Pt addition and HC-oxidation effects.



## 6. Acknowledgements

This work has been performed as part of the MISTRA (The Foundation for Strategic Environmental Research) funded program E4 (Energy Efficient Reduction of Exhaust Emissions from Vehicles), within the Competence Centre for Catalysis (KCK). KCK is financially supported by Chalmers University of Technology, the Swedish Energy Agency and the member companies: AB Volvo, Volvo Car Corporation AB, Scania CV AB, Haldor Topsøe A/S and ECAPS AB. Financial support from Knut and Alice Wallenberg Foundation, Dnr KAW 2005.0055, and Area of Advance Transport are gratefully acknowledged.

I would also like to thank the following persons who has helped in the process of this thesis:

Associate Professor **Hanna Härelind**, my friend and main supervisor, who always takes the time to discuss everything from science to the world in general. Thanks for everything!

Professor **Magnus Skoglundh**, my supervisor and examiner who, despite his many obligations and busy schedule, always finds time to help and encourage.

Dr **Hannes Kannisto**, roommate, friend, gym buddy and fellow beer aficionado, who laid the ground work for the thesis. Thanks for all the help and for making work feel like such a fun place!

Tekn. Lic. **Simon Klacar**, associate professor **Anders Hellman** and associate professor **Henrik Grönbeck**, for all the help and for keeping my ideas within the chemically legal limits.

**Carl Wadell** at Chemical Physics, Department of Applied Physics, Chalmers University of Technology, is greatly acknowledged for his assistance with the UV-vis measurements.

To all the **colleagues** and friends at TYK and KCK for filling the days with interesting discussions and for filling the Fridays evening with great company.

To my **parents** and **sister**, for the all the encouragement over the years!

To **Emma**, how crossed the sea to brighten my world!



## 7. List of abbreviations

AdBlue	Urea-solution (32% urea in water)
BE	Binding energy
BET	Brunauer-Emmet-Teller, method for determining SSA
CEM	Controlled evaporator mixer
DEF	Diesel Exhaust Fluid
EGR	Exhaust gas recirculation
FTIR	Fourier transformed infrared spectroscopy
HC	Hydrocarbon
ID	Inner diameter
L	Length
OD	Outer diameter
NO <sub>x</sub>	Nitrogen oxides (NO+NO <sub>2</sub> )
TWC	Three-Way-Catalyst
PGM	Platinum Group Metals
SSA	Specific surface area
SCR	Selective catalytic reduction
UV-vis	Ultraviolet-visual spectroscopy
XPS	X-ray photoelectron spectroscopy



## 8. References

1. Chorkendorff, I. and Niemantsverdriet, J.W., *Concepts of Modern Catalysis and Kinetics*. 2 ed 2007, Weinheim: Wiley-VCH.
2. Detels, R., Tashkin, D.P., Sayre, J.W., Rokaw, S.N., Massey, F.J., Coulson, A.H. and Wegman, D.H., *The UCLA population studies of CORD: X. A cohort study of changes in respiratory function associated with chronic exposure to SO<sub>x</sub>, NO<sub>x</sub>, and hydrocarbons*. American Journal of Public Health, 1991. **81**(3): p. 350-359.
3. Price, D., Birnbaum, R., Batiuk, R., McCullough, M. and Smith, R., *Nitrogen oxides: Impacts on public health and the environment*, in *Other Information: PBD: Aug 1997*1997. p. Medium: P; Size: 165 p.
4. European Parliament, C., *Regulation (EC) No 715/2007* 2007.
5. Matsumoto, S.i., *Catalytic Reduction of Nitrogen Oxides in Automotive Exhaust Containing Excess Oxygen by NO<sub>x</sub> Storage-Reduction Catalyst*. CATTECH, 2000. **4**(2): p. 102-109.
6. Zheng, M., Reader, G.T. and Hawley, J.G., *Diesel engine exhaust gas recirculation—a review on advanced and novel concepts*. Energy Conversion and Management, 2004. **45**(6): p. 883-900.
7. Skalska, K., Miller, J.S. and Ledakowicz, S., *Trends in NO<sub>x</sub> abatement: A review*. Science of The Total Environment, 2010. **408**(19): p. 3976-3989.
8. Dawody, J., Skoglundh, M., Wall, S. and Fridell, E., *Role of Pt-precursor on the performance of Pt/BaCO<sub>3</sub>/Al<sub>2</sub>O<sub>3</sub>-NO<sub>x</sub> storage catalysts*. Journal of Molecular Catalysis A: Chemical, 2005. **225**(2): p. 259-269.
9. Epling, W.S., Campbell, L.E., Yezerets, A., Currier, N.W. and Parks, J.E., *Overview of the Fundamental Reactions and Degradation Mechanisms of NO<sub>x</sub> Storage/Reduction Catalysts*. Catalysis Reviews, 2004. **46**(2): p. 163-245.
10. Kapoor, M., *Diesel Emissions Conference India 2011*. Platinum Metals Review, 2012. **56**(1): p. 36-39.
11. Iwamoto, M., Yahiro, H., Yu-u, Y., Shundo, S. and Mizuno, N., *Selective reduction of NO by lower hydrocarbons in the presence of O<sub>2</sub> and SO<sub>2</sub> over copper ion-exchanged zeolites*. Shokubai, 1990. **32**(6): p. 430-433.
12. Held, W., Koenig, A., Richter, T. and Puppe, L., *Society of Automobile Engineers*. Technical Paper Series, 1990. **900496**.
13. Burch, R., *Knowledge and know-how in emission control for mobile applications*. Catalysis Reviews - Science and Engineering, 2004. **46**(3-4): p. 271-333.
14. Miyadera, T., *Alumina-supported silver catalysts for the selective reduction of nitric oxide with propene and oxygen-containing organic compounds*. Applied Catalysis B: Environmental, 1993. **2**(2-3): p. 199-205.
15. Itoh, Y., Ueda, M., Shinjoh, H., Sugiura, M. and Arakawa, M., *NO<sub>x</sub> reduction behavior on alumina with discharging nonthermal plasma in simulated oxidizing exhaust gas*. Journal of Chemical Technology & Biotechnology, 2006. **81**(4): p. 544-552.
16. Narula, C.K., Daw, C.S., Hoard, J.W. and Hammer, T., *Materials Issues Related to Catalysts for Treatment of Diesel Exhaust*. International Journal of Applied Ceramic Technology, 2005. **2**(6): p. 452-466.
17. Burch, R., Fornasiero, P. and Watling, T., *Kinetics and Mechanism of the Reduction of NO by n-Octane over Pt/Al<sub>2</sub>O<sub>3</sub> under Lean-Burn Conditions*. Journal of Catalysis, 1998. **176**(1): p. 204-214.
18. Arve, K., Klingstedt, F., Eränen, K., Wärnå, J., Lindfors, L.E. and Murzin, D.Y., *Kinetics of NO<sub>x</sub> reduction over Ag/alumina by higher hydrocarbon in excess of oxygen*. Chemical Engineering Journal, 2005. **107**(1): p. 215-220.
19. Arve, K., Carucci, J.R.H., Eränen, K., Aho, A. and Murzin, D.Y., *Kinetic behaviour of HC-SCR over Ag/alumina catalyst using a model paraffinic second generation biodiesel compound*. Applied Catalysis B: Environmental, 2009. **90**(3-4): p. 603-612.

20. Arve, K., Eränen, K., Snåre, M., Klingstedt, F. and Murzin, D., *Selective catalytic reduction of NO<sub>x</sub> over Ag/Al<sub>2</sub>O<sub>3</sub> using various bio-diesels as reducing agents*. Topics in Catalysis, 2007. **42-43**(1): p. 399-403.
21. Shimizu, K., Kawabata, H., Satsuma, A. and Hattori, T., *Formation and reaction of surface acetate on Al<sub>2</sub>O<sub>3</sub> during NO reduction by C<sub>3</sub>H<sub>6</sub>*. Applied Catalysis B-Environmental, 1998. **19**(2): p. L87-L92.
22. Bion, N., Saussey, J., Haneda, M. and Daturi, M., *Study by in situ FTIR spectroscopy of the SCR of NO, by ethanol on Ag/Al<sub>2</sub>O<sub>3</sub> - Evidence of the role of isocyanate species*. Journal of Catalysis, 2003. **217**(1): p. 47-58.
23. Burch, R., Breen, J.P., Hill, C.J., Krutzsch, B., Konrad, B., Jobson, E., Cider, L., Eranen, K., Klingstedt, F. and Lindfors, L.E., *Exceptional activity for NO<sub>x</sub> reduction at low temperatures using combinations of hydrogen and higher hydrocarbons on Ag/Al<sub>2</sub>O<sub>3</sub> catalysts*. Topics in Catalysis, 2004. **30-31**(1-4): p. 19-25.
24. Shi, X., Yu, Y., He, H., Shuai, S., Dong, H. and Li, R., *Combination of biodiesel-ethanol-diesel fuel blend and SCR catalyst assembly to reduce emissions from a heavy-duty diesel engine*. Journal of Environmental Sciences, 2008. **20**(2): p. 177-182.
25. Satokawa, S., *Enhancing the NO/C<sub>3</sub>H<sub>8</sub>/O<sub>2</sub> Reaction by Using H<sub>2</sub> over Ag/Al<sub>2</sub>O<sub>3</sub> Catalysts under Lean-Exhaust Conditions*. Chemistry Letters, 2000. **29**(3): p. 294.
26. Breen, J.P., Burch, R., Hardacre, C. and Hill, C.J., *Structural investigation of the promotional effect of hydrogen during the selective catalytic reduction of NO<sub>x</sub> with hydrocarbons over Ag/Al<sub>2</sub>O<sub>3</sub> catalysts*. Journal of Physical Chemistry B, 2005. **109**(11): p. 4805-4807.
27. Breen, J.P. and Burch, R., *A review of the effect of the addition of hydrogen in the selective catalytic reduction of NO<sub>x</sub> with hydrocarbons on silver catalysts*. Topics in Catalysis, 2006. **39**(1-2): p. 53-58.
28. Shibata, J., Shimizu, K., Satokawa, S., Satsuma, A. and Hattori, T., *Promotion effect of hydrogen on surface steps in SCR of NO by propane over alumina-based silver catalyst as examined by transient FT-IR*. Physical Chemistry Chemical Physics, 2003. **5**(10): p. 2154-2160.
29. Miyadera, T., *Alumina-supported silver catalyst for the selective reduction of nitric-oxide with propene and oxygen-containing organic compounds*. Applied Catalysis B-Environmental, 1993. **2**(2-3): p. 199-205.
30. Arve, K., Backman, H., Klingstedt, F., Eränen, K. and Murzin, D.Y., *Kinetic considerations of H<sub>2</sub> assisted hydrocarbon selective catalytic reduction of NO over Ag/Al<sub>2</sub>O<sub>3</sub>: I. Kinetic behaviour*. Applied Catalysis A: General, 2006. **303**(1): p. 96-102.
31. Kannisto, H., Karatzas, X., Edvardsson, J., Pettersson, L.J. and Ingelsten, H.H., *Efficient low temperature lean NO<sub>x</sub> reduction over Ag/Al<sub>2</sub>O<sub>3</sub>—A system approach*. Applied Catalysis B: Environmental, 2011. **104**(1-2): p. 74-83.
32. Kannisto, H., Ingelsten, H.H. and Skoglundh, M., *Ag-Al<sub>2</sub>O<sub>3</sub> catalysts for lean NO<sub>x</sub> reduction-- Influence of preparation method and reductant*. Journal of Molecular Catalysis A: Chemical, 2009. **302**(1-2): p. 86-96.
33. Kannisto, H., Arve, K., Pingel, T., Hellman, A., Harelind, H., Eranen, K., Olsson, E., Skoglundh, M. and Murzin, D.Y., *On the performance of Ag/Al<sub>2</sub>O<sub>3</sub> as HC-SCR catalyst - influence of silver loading, morphology and nature of the reductant*. Catalysis Science & Technology, 2012, DOI: 10.1039/C2CY20594G.
34. Härelind, H., Gunnarsson, F., Vaghefi, S.M.S., Skoglundh, M. and Carlsson, P.-A., *Influence of the Carbon-Carbon Bond Order and Silver Loading on the Formation of Surface Species and Gas Phase Oxidation Products in Absence and Presence of NO<sub>x</sub> over Silver-Alumina Catalysts*. ACS Catalysis, 2012. **2**(8): p. 1615-1623.
35. Shibata, J., Takada, Y., Shichi, A., Satokawa, S., Satsuma, A. and Hattori, T., *Ag cluster as active species for SCR of NO by propane in the presence of hydrogen over Ag-MFI*. Journal of Catalysis, 2004. **222**(2): p. 368-376.

36. Shimizu, K., Shibata, J. and Satsuma, A., *Kinetic and in situ infrared studies on SCR of NO with propane by silver-alumina catalyst: Role of H<sub>2</sub> on O<sub>2</sub> activation and retardation of nitrate poisoning*. Journal of Catalysis, 2006. **239**(2): p. 402-409.
37. Kung, M. and Kung, H., *Lean NO<sub>x</sub> catalysis over alumina supported catalysts*. Topics in Catalysis, 2000. **10**(1-2): p. 21-26.
38. She, X. and Flytzani-Stephanopoulos, M., *The role of Ag-O-Al species in silver-alumina catalysts for the selective catalytic reduction of NO<sub>x</sub> with methane*. Journal of Catalysis, 2006. **237**(1): p. 79-93.
39. Meunier, F.C., Breen, J.P., Zuzaniuk, V., Olsson, M. and Ross, J.R.H., *Mechanistic aspects of the selective reduction of NO by propene over alumina and silver-alumina catalysts*. Journal of Catalysis, 1999. **187**(2): p. 493-505.
40. Bethke, K.A. and Kung, H.H., *Supported Ag catalysts for the lean reduction of NO with C<sub>3</sub>H<sub>6</sub>*. Journal of Catalysis, 1997. **172**(1): p. 93-102.
41. Shi, C., Cheng, M.J., Qu, Z.P. and Bao, X.H., *Investigation on the catalytic roles of silver species in the selective catalytic reduction of NO<sub>x</sub> with methane*. Applied Catalysis B-Environmental, 2004. **51**(3): p. 171-181.
42. Liu, Z.M. and Woo, S.I., *Recent advances in catalytic DeNO<sub>x</sub> science and technology*. Catalysis Reviews - Science and Engineering, 2006. **48**(1): p. 43-89.
43. van Santen, R., *M. Neurock in G. Ertl, H. Knözinger, J. Weitkamp (eds.): Handbook of Heterogeneous Catalysis, Vol. 3, 1997, Wiley-VCH, Weinheim*.
44. Brunauer, S., Emmet P. H., Teller E., *Adsorption of gases in multimolecular layers*. Journal of the American Chemical Society, 1938. **60**: p. 309-319.
45. Michael, B., *The basis and applications of heterogenous catalysis*1998: Oxford Press.
46. Kittel, C., *Introduction to Solid State Physics*. 8th edition ed2005: John Wiley & Sons.
47. Moulder, J.F., W. F. Stickle, P. E. Sobol, K. D. Bomben, *Handbook of X-Ray Photoelectron Spectroscopy*, ed. Chastain, J.1992, Eden Prairie: Perkin Elmer Corporation - Physical Electronics Division.
48. Imelik, B. and Védrine, J.C., *Catalyst characterization: physical techniques for solid materials*1994: Springer.
49. Rantanen, L., Linnaila, R., Aakko, P. and Harju, T., *NExBTL-Biodiesel fuel of the Second Generation*. SAE, 2005. **2005-01-377**.
50. Atkins, P. and Jones, L., *Chemical principles*2006: WH Freeman.
51. Harris, D.C., *Quantitative chemical analysis*2006: WH Freeman.
52. Bogdanchikova, N., Meunier, F.C., Avalos-Borja, M., Breen, J.P. and Pestryakov, A., *On the nature of the silver phases of Ag/Al<sub>2</sub>O<sub>3</sub> catalysts for reactions involving nitric oxide*. Applied Catalysis B: Environmental, 2002. **36**(4): p. 287-297.
53. Pestryakov, A.N. and Davydov, A.A., *Study of supported silver states by the method of electron spectroscopy of diffuse reflectance*. Journal of Electron Spectroscopy and Related Phenomena, 1995. **74**(3): p. 195-199.
54. Bukhtiyarov, V., Kaichev, V. and Prosvirin, I., *Oxygen adsorption on Ag (111): X-ray photoelectron spectroscopy (XPS), angular dependent x-ray photoelectron spectroscopy (ADXPS) and temperature-programmed desorption (TPD) studies*. The Journal of chemical physics, 1999. **111**(5): p. 2169-2175.
55. Manna, A., Kulkarni, B.D., Bandyopadhyay, K. and Vijayamohanan, K., *Synthesis and Characterization of Hydrophobic, Aprotically-Dispersible, Silver Nanoparticles in Winsor II Type Microemulsions*. Chemistry of Materials, 1997. **9**(12): p. 3032-3036.
56. Lindfors, L.E., Eranen, K., Klingstedt, F. and Murzin, D.Y., *Silver/alumina catalyst for selective catalytic reduction of NO<sub>x</sub> to N<sub>2</sub> by hydrocarbons in diesel powered vehicles*. Topics in Catalysis, 2004. **28**(1-4): p. 185-189.
57. Li, W.-X., Stampfl, C. and Scheffler, M., *Why is a Noble Metal Catalytically Active? The Role of the O-Ag Interaction in the Function of Silver as an Oxidation Catalyst*. Physical Review Letters, 2003. **90**(25): p. 256102.

58. Shimizu, K., Shibata, J., Yoshida, H., Satsuma, A. and Hattori, T., *Silver-alumina catalysts for selective reduction of NO by higher hydrocarbons: structure of active sites and reaction mechanism*. Applied Catalysis B-Environmental, 2001. **30**(1-2): p. 151-162.
59. Siegbahn, P.E.M., *The activation of the C-H bond in acetylene by second row transition metal atoms*. Theoretica chimica acta, 1994. **87**(4-5): p. 277-292.
60. Träskelin, P., Saresoja, O. and Nordlund, K., *Molecular dynamics simulations of C<sub>2</sub>, C<sub>2</sub>H, C<sub>2</sub>H<sub>2</sub>, C<sub>2</sub>H<sub>3</sub>, C<sub>2</sub>H<sub>4</sub>, C<sub>2</sub>H<sub>5</sub>, and C<sub>2</sub>H<sub>6</sub> bombardment of diamond (1 1 1) surfaces*. Journal of Nuclear Materials, 2008. **375**(2): p. 270-274.
61. Bligaard, T., Nørskov, J.K., Dahl, S., Matthiesen, J., Christensen, C.H. and Sehested, J., *The Brønsted–Evans–Polanyi relation and the volcano curve in heterogeneous catalysis*. Journal of Catalysis, 2004. **224**(1): p. 206-217.
62. Bronsted, J.N., *Acid and Basic Catalysis*. Chemical Reviews, 1928. **5**(3): p. 231-338.
63. Evans, M.G. and Polanyi, M., *Inertia and driving force of chemical reactions*. Transactions of the Faraday Society, 1938. **34**(0): p. 11-24.
64. Vojvodic, A., Calle-Vallejo, F., Guo, W., Wang, S., Toftelund, A., Studt, F., Martinez, J.I., Shen, J., Man, I.C., Rossmeisl, J., Bligaard, T., Norskov, J.K. and Abild-Pedersen, F., *On the behavior of Brønsted-Evans-Polanyi relations for transition metal oxides*. The Journal of chemical physics, 2011. **134**(24): p. 244509.
65. Ruth, K., Burch, R. and Kieffer, R., *Mo–V–Nb Oxide Catalysts for the Partial Oxidation of Ethane: II. Chemical and Catalytic Properties and Structure Function Relationships*. Journal of Catalysis, 1998. **175**(1): p. 27-39.
66. Arve, K., Klingstedt, F., Eranen, K., Lindfors, L.E. and Murzin, D.Y., *Engineering HC-SCR: Improved low temperature performance through a cascade concept*. Catalysis Letters, 2005. **105**(3-4): p. 133-138.
67. Creaser, D., Kannisto, H., Sjöblom, J. and Ingelsten, H.H., *Kinetic modeling of selective catalytic reduction of NO<sub>x</sub> with octane over Ag–Al<sub>2</sub>O<sub>3</sub>*. Applied Catalysis B: Environmental, 2009. **90**(1–2): p. 18-28.
68. Meunier, F.C. and Ross, J.R.H., *Effect of ex situ treatments with SO<sub>2</sub> on the activity of a low loading silver-alumina catalyst for the selective reduction of NO and NO<sub>2</sub> by propene*. Applied Catalysis B-Environmental, 2000. **24**(1): p. 23-32.